Journal of Applied Mathematics and Physics, 2025, 13(10), 3352-3392
https://www.scirp.org/journal/jamp
ISSN Online: 2327-4379
ISSN Print: 2327-4352

Isothermal Magnetostrictive Convection

George Samuel Levy

Entropic Power, Irvine, CA, USA
Email: glevy#entropicpower.com

How to cite this paper: Levy, G.S. (2025) Isothermal Magnetostrictive Convection. *Journal of Applied Mathematics and Physics*, **13**, 3352-3392.
https://doi.org/10.4236/jamp.2025.1310193

Received: September 19, 2025
Accepted: October 26, 2025
Published: October 29, 2025

Abstract

Stereo-magnetostrictive fluids convect under the influence of a magnetic field and gravity. When a field is applied to one side of a tubular loop containing such fluid, but not to the other side, the fluid convects isothermally. The process is analogous to thermal convection except that the field replaces the temperature difference between heat source and heat sink. Forces that may retard convection are either dissipative or conservative. Dissipative forces produced by viscosity and hysteresis are flow-velocity dependent. They can slow down convection but cannot stop it. They can also be reduced by increasing the dimensions of the system. Conservative forces such as magnetic potential do create a potential barrier, but this barrier does not help or hinder convection because the fluid gains as much energy descending it as it loses climbing it. The thermodynamic cycle shows that ambient heat is converted to mechanical energy, thereby decreasing the entropy of the surroundings. This phenomenon falls outside the framework of applicability of the second law, which, as specified by all H-theorems, is limited to systems that are time-reversal symmetric at the microscopic scale. A proposed experiment for testing this theory is expected to produce an observable convective flow of about 0.375 to 1 mm/sec with a 20 cm high device. The device produces maximum power when it operates at the thermodynamic threshold where the measure of asymmetry is matched to the measure of symmetry. Additional information generated by magnetic time-reversal symmetry breaking is accounted for by adding an anomalous term to conventional entropy.

Keywords

Magnetostriction, CPT Symmetry, $E \times B$ Thermoelectric Effect, Convection, Spin Cross-Over

1. Introduction

Isothermal stereo-magnetostriction is an incontrovertible experimental fact. Hundreds of independent researchers have confirmed that in the presence of a mag-

netic field, spin cross-over causes stereo-magnetostrictive fluids to *change volume and density without any change in temperature* [1]-[46]. This extraordinary property implies the highly paradoxical phenomenon of *isothermal* convection. Under the influence of gravity, such a fluid in a tubular loop would circulate when one side of the loop is exposed to a *static* field. Given that both the field and gravity are *static*, it is also implied that the energy driving this convection cannot originate from the field or from gravity. Is such a phenomenon possible? What is the source of energy that drives convection?

This paper explores the thermodynamics of magnetostrictive heat engines. One can distinguish two kinds of materials that differ in the way they change shape.

Joule magnetostrictive [1] materials change shape but not volume, lengthening or shortening along the field direction and respectively shortening or lengthening in the perpendicular plane. They include Gerfenol-D, Terfenol-D, nickel, iron-gallium (Galfenol), and cobalt ferrites. They are utilized in various applications where precise control of dimensions is required, such as positioning, vibration control, and sound generation [2]-[6].

Stereo-magnetostrictive materials [7]-[46] rely on spin cross-over to change volume when exposed to a magnetic field. They switch from a low spin (LS) state in which few electrons are unpaired, to a high spin (HS) state, in which many are unpaired. This electronic reconfiguration alters the bond lengths and angles, which results in a reorganization of the lattice structure and ultimately leads to a macroscopic change in shape as well as volume. Many of these materials include iron(II) and iron(III) complexes, as shall be discussed in Section 7. When these materials are in a liquid phase, the magnetically induced volume changes and density gradients result in isothermal convection current.

In view of the controversial topic being covered, the author thought it prudent to be as precise and thorough as possible and perhaps, as a result, overly elementary in places. The following paragraphs provide a section-by-section summary of the arguments made in this paper:

Section 2 (Thought experiment of a stereo-magnetostrictive convection engine) describes a thought experiment involving a magnetostrictive fluid.

1) A stereo-magnetostrictive fluid filling a U-shaped tube undergoes a magnetostrictive change in volume and density on one side of the tube when this side is exposed to a magnetic field.

2) As required by hydrostatics, the fluid reaches a two-level equilibrium state, *i.e.*, acquires a pressure head.

3) Connecting the ends of the U-tube causes the fluid to flow from the high level to the low level. This flow can drive a turbine to convert potential energy to work.

4) The two-level equilibrium state disturbed by the turbine is restored by the fluid moving around the bottom of the loop, as required by hydrostatics.

Section 3 (Itemization of all forces in magnetic convection) explores all possible retarding effects that could stop convection, such as magnetic, viscous, and hyster-

etic forces and shows that they can be ignored.

1) All conservative forces in the form of a magnetic potential produce an energy barrier, but the energy spent going up is equal to the energy going down. These forces can neither add nor subtract energy from convection.

2) All dissipative viscous, including Newtonian viscous flow, hysteretic effects, and yield stress forces, are flow dependent. They may slow down, convection, but cannot stop it.

3) From a foundational thermodynamic perspective, the speed of convection is not as important as its very existence.

Section 4 (Force balance equation):

1) In an open circuit mode (turbine with zero conductance), all viscous forces are zero and all potential energy barriers cancel out. Therefore, the convective force F_{conv} is opposed by the force F_{load} across the load, *i.e.*, $F_{conv} = F_{load}$.

2) When the loop is closed, the fluid starts to flow and eventually reaches an equilibrium flow velocity v_{Flow}. At that point $F_{conv} = F_{load} + F_{visc}$.

3) Maximum power output is achieved by source-load matching the viscous force F_{visc} to the load force F_{load}, resulting in $F_{conv} = 2F_{load} = 2F_{visc}$.

Section 5 (The magnetostrictive cycle: the source of energy that drives convection) discusses the thermodynamic cycle of the magnetostrictive engine, showing that stereo-magnetostrictive convection decreases entropy and that the energy driving convection comes from the thermal energy of the fluid.

1) This circulation is powered by the magnetostrictive volume changes $+\Delta V$ at high pressure $p_0 + \Delta p$ at the bottom of the loop, and $-\Delta V$ at low pressure p_0 at the top. The process is endothermic, converting heat to work, *i.e.*, $Q = W = \Delta p \Delta V$.

2) This process can be run continuously by extracting heat isothermally from a heat bath, thereby lowering its entropy by $\Delta S = -\Delta Q / T$.

3) The process is an entropic effect *in which ΔS is the change in entropy ΔS associated with spin cross-over between Low Spin and High Spin*.

Section 6 (Framework of applicability of second law): The second law is not universal.

1) The framework of applicability of the second law is limited by the assumption made in all formulations of the H-theorem that all microscopic interactions are time-reversal symmetric. In contrast, the magnetic convection described in this paper relies on the magnetic field, which is CPT (Charge-Parity-Time) symmetric, and, therefore, falls outside this framework.

2) Kelvin-Planck formulation of the law is empirical and based on a large number of experiments. However, no experiment comparable to the one presented herein has been conducted under the specific conditions of isothermal operation with magnetostrictive materials in the presence of static magnetic fields and gravity.

Therefore, the law is not violated, it is bypassed. It remains valid within its domain of applicability.

Section 7 (Proposed experiment) describes a proposed experiment for testing

the theory advanced in this paper. It includes a brief overview of different stereo-magnetostrictive materials as well as a proposed design for a realistic convection engine.

1) The predicted convection velocity for this experiment of about 1 mm/sec provides a testable prediction that can experimentally validate or refute these theoretical claims.

2) This process may be slow *but from a foundational thermodynamics point of view, speed is not as significant as the very existence of convection. This is the whole purpose of this thought experiment*.

Section 8 (Operating at the thermodynamic threshold to maximize performance) discusses the thermodynamic threshold optimization method that maximizes the power output by matching a measure of the asymmetry to a measure of background symmetrical processes.

1) Time-reversal asymmetric phenomena are difficult to observe because they occur against a time-symmetric background "noise".

2) To maximize their thermodynamic impact, they should be commensurate with this background. If they are too small, the background dominates, and they cease to be observable.

3) Conversely, if the background symmetric processes are too small, they are unable to provide sufficient energy to drive thermal conversion and there is no thermodynamic impact.

4) Maximum performance is achieved at the thermodynamic threshold, at which both kinds of processes have equal measures.

Section 9 (Suggested extension of second law and entropy to include symmetry-breaking phenomena) explores extensions of the second law that cover time-reversal symmetry-breaking phenomena.

1) The time-reversal symmetry assumption of conventional thermodynamics implies redundancy: the same information describes forward and reverse dynamics, thereby making reversible processes possible.

2) The breaking of the time-reversal symmetry by the CPT symmetry of the magnetic field adds states not accounted for by conventional entropy, but that uniquely determine the direction of a process, thereby rendering reversibility impossible.

3) It is therefore suggested that entropy should comprise two components: the first, S_A, to represent conventional entropy bound by the H-theorem, $dS_A/dt \geq 0$, and the second, S_B, to represent the additional information generated by the breaking of time-reversal symmetry.

A list of symbols can be found in **Appendix 1**.

2. Thought Experiment of a Stereo-Magnetostrictive Convection Engine

Consider a tubular loop filled with a stereo-magnetostrictive fluid. The fluid consists of small stereo-magnetostrictive particles in a solvent. The loop is oriented

vertically in a gravitational field as shown in Figure 1 and a magnetic field is applied to the right column of the loop.

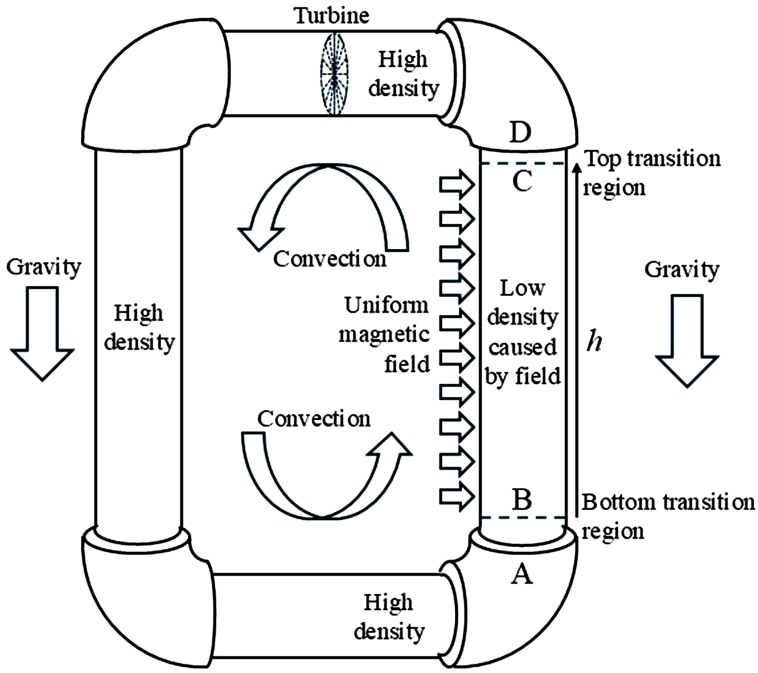

Figure 1. Thought experiment of a stereo-magnetostrictive engine. A magnetic field and gravity in combination cause the convection of a stereo-magnetostrictive fluid without the need for a temperature gradient.

For the sake of simplicity and clarity, the following shall be assumed:

1) The field *B is time invariant and spatially uniform* along the height *h* of the magnetized region on the right-hand side. *This field is produced by a permanent magnet and does not require a continuous input of energy* to be maintained.

2) The field drops from its uniform value to zero in two transition regions at the top and bottom of the magnetized region.

3) The fluid is ideally magnetostrictive, that is, its volumetric strain ratio $\Delta V/V$ changes linearly with a magnetic field B:

$$K_m B = \left(\frac{\Delta V}{V}\right) \approx -\left(\frac{\Delta \rho}{\rho}\right) \tag{1}$$

where K_m is the material-dependent magnetostrictive volume ratio modulus.

4) There is no hysteresis. As shall be justified in Section 3.4 (Hysteretic viscous force) hysteresis is not significant in a physical implementation.

5) The magnetostrictive fluid is considered to be an ideal liquid, incompressible by gravitational pressure. This assumption is justified by real world data, which shows that compressibility by gravity of different physical fluids can be neglected (see Section 7, Material Selection Requirements). As an example, for $Fe(NH_2trz)_{32}$, the change in volume due to the magnetic field is six orders of magnitude larger than the one due to gravity.

6) The process is in contact with a heat bath and is isothermal. Any change in volume due to a temperature change is ruled out. Therefore, convection is entirely due to the magnetic field and is neither aided nor retarded by any temperature gradient.

In accordance with their stereo-magnetostriction property, fluid particles in the magnetized column increase their volume, causing the fluid to decrease in density. In the demagnetized column, particles return to their normal volume, and the fluid to its normal density. The difference in density between the two sides causes the fluid to convect around the loop. A turbine inserted in the loop can convert this flow to electrical energy. This phenomenon clearly falls outside of conventional thermodynamics.

Onsager excluded magnetic fields from his reciprocals because he thought with good reason that the fields could produce effects forbidden by the second law, for example isothermal convection. We are left with two choices:

1) Simply ignore the paradox and refrain from associating reciprocals with magnetic fields. This is the approach taken by Onsager.

2) Tackle the paradox head on and see where it leads us. This is the approach taken in this paper.

3. Itemization of All Forces in Magnetic Convection

Our first concern is to itemize all forces to eliminate the possibility of retarding effects prohibiting convection. Forces and effects that affect magnetic convection include:

1) Forward force convective force F_{conv}.

2) Backward load force F_{load}.

3) Newtonian viscous force F_{visc_Newton}.

4) Hysteretic viscous force F_{visc_hyst}.

5) Static magnetic potential barrier force F_{magn}.

6) Yield shear stress force.

7) Static friction force.

8) Molecular aggregation and separation from solvent.

Table 1 provides an outline of the characteristics of each force.

Table 1. Summary of forces involved in magnetic convection.

Convective force F_{conv}	Physics	Magnetostriction, hydrostatics.
	Cause	Density difference $\Delta\rho$ due to magnetic field.
	Effect	Convective pressure $p_{conv} = (\rho g n K_m B) h$.
	Optimize	Increase K_m, B, and h.
Backward load force F_{load}	Physics	Conversion of potential energy to mechanical energy.
	Cause	Turbine.
	Effect	Produces back force F_{load} and power $P_{load} = v_{Flow} F_{load}$.
	Optimize	Use source/load matching: $F_{load} = F_{visc} = 1/2 F_{conv}$.

Continued

Newtonian viscous forces F_{visc_Newton}	Physics	Dissipative, viscous, flow-dependent.
	Cause	Friction.
	Effect	Slowdown by back pressure $p_{visc\_Newton} = 8\eta L v_{Flow}/r^2$.
	Remedy	Increase r.
Hysteretic viscous force F_{visc_hyst}	Physics	Dissipative, viscous, flow-dependent.
	Cause	Hysteresis lag in flowing fluid breaks vertical symmetry of density distribution; enables gradient force $\mu_{magn}\nabla B$. Relaxation time in μsec.
	Effect	Slowdown in transition zones; second order effect; small in view of slow system time constant (seconds).
	Remedy	Small, can be neglected; if needed increase h; decrease μ_{magn}; increase system time constant.
Yield shear stress rheological effect	Physics	Dissipative.
	Cause	Rheological effect, dipole to dipole chaining.
	Effect	Yield stress stops flow.
	Remedy	Increase shear stress by increasing r.
Static magnetic potential barrier F_{magn}	Physics	Conservative: $\oint\left(\mu_{magn}B\right)\mathrm{d}s = 0$.
	Cause	Stored potential magnetic energy in $\mu_{magn}B$.
	Effect	No net effect because of first law.
	Remedy	No remedy needed.
Molecule aggregation and separation of from solvent	Physics	Field driven.
	Cause	Drift due to $\mu_{magn}\nabla B$, gravity and intermolecular forces.
	Effect	Very small, $v_{drift} \approx v_{Brownian} \times 10^{-6}$.
	Remedy	Can be neglected; if needed apply surfactants, increase v_{Flow}, h, and r.
Static friction force	Physics	Dissipative when it slides, conservative when not.
	Cause	Surface irregularities, molecular adhesion.
	Effect	Only present when flow = 0. Cannot exist in liquids.
	Remedy	No remedy needed.

3.1. Forward Convective Force F_{conv}

This force is proportional to gravitational acceleration g, and the difference in mass Δm between the right-hand side and the left-hand side of the loop. Furthermore, Δm is proportional to the density of the fluid ρ, and the magnetostrictive change in volume ΔV. In addition, ΔV is a function of the magnetostrictive index K_m and the magnetic field B:

$$F_{conv} = g\Delta m = g\rho\Delta V = g\rho V K_m B \tag{2}$$

For a tube of height h and cross-sectional area $A=\pi r^2$, $V = \pi r^2 h$, the convective force is:

$$F_{conv} = \left(g\rho\pi r^2 K_m B\right)h \tag{3}$$

and the corresponding convective pressure is:

$$p_{conv} = \left(g\rho K_m B\right)h \tag{4}$$

Parentheses have been inserted in the above equations to emphasize that F_{conv} and p_{conv} are proportional to the height of the tube. This implies that F_{conv} can be made arbitrarily large by increasing h.

3.2. Backward Load Force F_{load}

The force is caused by the turbine inserted in the convection loop and is a function of the power P_{load} being generated and the flow velocity v_{Flow}.

$$F_{load} = \frac{P_{load}}{v_{Flow}} \tag{5}$$

3.3. Newtonian Viscous Force F_{visc_Newton}

This force is flow-dependent and occurs around the convection loop. Even though there is no experimental evidence of such, this force may include small reversible and flow-dependent rheological effects induced by the magnetic field. It can be derived for laminar flow using Poiseuille's law. For a given loop length L, a viscosity η of the fluid, a tube radius r, and a hydrostatic pressure p_{visc_Newton}, the volumetric flow Q_{Flow} is:

$$Q_{Flow} = \left(\frac{\pi p_{visc\_Newton}}{8\eta L}\right)r^4 \tag{6}$$

Assuming a circular cross-sectional area πr^2 and a flow velocity $v_{Flow} = Q_{Flow}/\pi r^2$, the back pressure produced by the viscous flow is:

$$p_{visc\_Newton} = \left(8\eta L\right)\frac{v_{Flow}}{r^2} \tag{7}$$

Parentheses have been inserted to clearly emphasize the dependency of p_{visc_Neton} on the radius r of the tube and on the flow velocity v_{Flow}. This pressure can always be made smaller by increasing r. Since $F_{visc\_Newton} = p_{visc\_Newton}\pi r^2$, the viscous force is:

$$F_{visc\_Newton} = 8\pi\eta L v_{Flow} \tag{8}$$

The possibility that Poiseuille's law does not apply because of turbulence is not a concern. In such a case, the high flow speed would make magnetic convection a well-established fact. This force can be mitigated by increasing the radius r of the convection tube as shown by Equation (7).

3.4. Hysteretic Viscous Force F_{visc_hyst}

This force is produced by hysteretic lag due to the flow of the magnetostrictive molecules. This lag breaks the vertical symmetry in the density of the molecules, thereby enabling the magnetic gradient force $\mu_{magn}\nabla B$ as explained below.

A molecule with a magnetic moment μ_{magn}, and subjected to a field experiences a force proportional to the field's gradient ∇B:

$$F_{Bmolecule} = \mu_{magn}\nabla B \tag{9}$$

Along the height of the magnetized tube the field is uniform, and this force is zero. However, in the magnetic transition regions at the top and bottom of the magnetized tube, the field decreases to zero, implying two symmetrical non-zero gradients. In these locations, the field exerts a force $\mu_{magn}\nabla B$ on a molecule at the bottom transition zone and $-\mu_{magn}\nabla B$ on a molecule at the top. The sum of all forces for both zones are given by:

$$F_B = \sum_{i}^{Bottom} \left(\mu_{magn}\nabla B\right)_i + \sum_{j}^{Top} \left(\mu_{magn}\nabla B\right)_j \tag{10}$$

where $(\mu_{magn}\nabla B)_i$ and $(\mu_{magn}\nabla B)_j$ are functions of the position of each molecule with respect the field gradient.

The density of the fluid is not affected by gravity because the fluid is not compressible by gravitational pressure. However, being magnetostrictive, its density changes around the loop, uniformly less dense in the magnetized section, uniformly denser in the non-magnetized section and gradually changing in the transition zones.

In the no-flow static equilibrium state, the density profiles, $\mathrm{d}N/\mathrm{d}h$, in the top and bottom zones are exactly symmetrical, decreasing at the bottom, and increasing symmetrically at the top, *i.e.*, $(-\mathrm{d}N/\mathrm{d}h)_{\mathrm{Bottom}} = (+\mathrm{d}N/\mathrm{d}h)_{\mathrm{Top}}$. Given this symmetry in density, and symmetry of the field gradients ∇B, all gradient forces $\mu_{magn}\nabla B$ exerted on molecules at the top and bottom add up to zero.

$$F_B = \sum_{Bottom} \mu_{magn}\nabla B + \sum_{top} \mu_{magn}\nabla B = 0 \tag{11}$$

As the fluid flows through the transition zones, the magnetostrictive effect causes molecular spin states to change. Any lag in this process breaks the symmetry of the density profile causing Equation (11) to be non-zero.

Hysteretic drag is a small second order effect that manifests itself as a tiny flow-dependent viscous resistance restricted to the transition regions. However, if necessary, it can be remedied in two ways.

1) Being restricted to the transition zones, it is independent of height and therefore can be countered by increasing the height h of the convection loop, thereby increasing the convective driving force F_{conv} relatively to F_{visc_hyst}.

2) It can also be rendered ineffective by increasing the time constant of the system. Its relaxation time is determined by the probability of a molecule transitioning back to its lowest energy level. For a spin cross-over molecule this relaxation time is in the order of microseconds (see **Tables 2(a)-(c)** and [45] [46]). This time is significantly shorter than the passage of molecules through the magnetic transition zone AB and CD in **Figure 1**. At a flow rate of 0.375 mm/sec as worked out in the example of Section 7, molecules would spend several seconds in the transition zones. In comparison, the spin relaxation time is 10 - 200 μsec or about three orders of magnitude faster, thereby making the hysteretic lag irrelevant. However, if necessary, this effect can be countered by increasing the time constant of the system.

Therefore, the no-hysteresis assumption made in the thought experiment is justified. In any case, since this force is viscous, it can only exist in the presence of convection. See Equation (3). Therefore, the very presence of this force is not an issue because its presence indicates convection, precisely the effect intended to be demonstrated.

3.5. Yield Shear Stress Force

If a rheological retarding force arises for whatever reason (for example magnetic dipole to dipole chaining, aggregation, or any other such effect), the resulting yield stress τ_{yield} of the fluid against the walls of the tube must be overcome by the shear stress τ_{shear} at the wall of the tube caused by the convective force F_{conv}. This force is proportional to τ_{shear} and to the convective pressure p_{conv}. For a loop of length L and a tube radius r, F_{conv} can be written as:

$$F_{conv} = 2\pi rL\tau_{shear} = \pi r^2 p_{conv} \tag{12}$$

Inserting the expression for p_{conv} from Equation (4) into Equation (12) yields:

$$2\pi rL\tau_{shear} = \pi r^2 g\rho K_m Bh \tag{13}$$

where h is the height of the tube. Simplifying and solving for τ_{shear}:

$$\tau_{shear} = \left(\frac{g\rho K_m B}{2}\right)\frac{h}{L}r \tag{14}$$

For convection to begin, the driving shear stress must exceed the fluid's yield stress τ_{yield}:

$$\tau_{shear} = \left(\frac{g\rho K_m B}{2}\right)\frac{h}{L}r > \tau_{yield} \tag{15}$$

Assuming that the length of the loop is twice its height, $L = 2h$, Equation (14) becomes:

$$\tau_{shear} = \left(\frac{g\rho K_m B}{4}\right)r > \tau_{yield} \tag{16}$$

Therefore, the driving shear stress is *proportional to the radius of the tube* and increasing r sufficiently can overcome any yield stress. The fluid then still flows, albeit with a greater viscosity and the flow-velocity dependent argument of Section 3.3 applies.

3.6. Static Magnetic Potential Barrier Force F_{magn}

Magnetic potential may have several origins. For example, it may be due to spin or orbital coupling, or to magnetic gradient interaction with dipoles.

Regardless of its origin, it is a conserved quantity that cannot contribute to nor hinder convection. Any loop integral of this potential must be zero. Being static and conservative, the magnetic field (as well as gravity) cannot add or subtract any net energy from the convective process. A departure from this principle would violate the first law of thermodynamics (see Note 1)).

Accordingly, a potential magnetic energy barrier does exist, but its net effect is zero and is not an obstacle to convection. As particles cross the bottom transition zone and get exposed to the field, they ascend this barrier and acquire magnetic potential energy. Conversely, as they cross the top transition zone, they exit the field, descend the barrier, and give up this energy to *return to their original state*. This exchange in magnetic potential energy cancels out as shown in the PV thermodynamic cycle of Section 5.

Another way of explaining this phenomenon, is that any conservative force produced in one transition zone is counterbalanced by a symmetrically opposite conservative force in the other transition zone. Being hydrostatically connected as in a chain, their contribution to convection is zero.

3.7. Static Friction Force

Static friction, arguably, could be considered either "conservative" or "dissipative". Nevertheless, it only occurs in solids, not in liquids. The 1/10 volume ratio of magnetostrictive molecules to solvent in the experiment of Section 7 precludes the solution from turning solid due to a rheological effect. Even if such a rheological effect did happen, it would only produce a slight increase in viscosity with a finite relaxation time. To my knowledge, no such effect has been observed in spin crossover materials.

3.8. Molecule Aggregation and Separation of from Solvent

One can also rule out as a no-go reason for magnetic convection, the separation of the magnetic molecules from their solution by the magnetic field. As explained in **Appendix 2** "Separation of SCO molecules by the magnetic field", given the size of the molecules, the viscosity of the solution, and the likely non-uniformity of the field, the displacement due to Brownian motion is about 20 microns in one second, while the separation drift due to the magnetic field is in the order of 20 picometers per second, a ratio approximately one million times smaller. This effect can also be reduced by adding surfactants to the solution.

Aggregation due to molecular attraction can be mitigated by adding surfactants and with higher fluid flow, which can be done by increasing the dimensions of the system.

4. Force Balance Equation

To simplify our notation, let us combine the Newtonian viscous force F_{visc_Newton} and the hysteretic viscous force F_{visc_hyst} into one:

$$F_{visc} = F_{visc\_Newton} + F_{visc\_hyst} \tag{17}$$

Since magnetic potential does not transfer energy to the fluid, it can be ignored. Therefore, all relevant forces can be expressed using Newton's law as:

$$F_{conv} - F_{load} - F_{visc} = ma \tag{18}$$

Now, consider an open circuit static equilibrium state, with $ma = 0$, and $v_{Flow} =$

0, and without any flow-dependent viscous force, *i.e.*, $F_{visc} = 0$. The only forces left are F_{conv} and F_{load}. Equation (18) reduces to:

$$F_{conv} = F_{load} \tag{19}$$

In other words, the convective drive is equal to the pressure head caused by difference in height between the left and right columns.

Now, consider closing the loop with a conductive load (*i.e.*, turbine). The fluid accelerates until it reaches a dynamic equilibrium at velocity v_{Flow} such that a viscous force F_{visc} is produced:

$$F_{conv} - F_{load} - F_{visc} = 0 \tag{20}$$

Using the source load matching technique, the power transfer to the load can be maximized, for example, by throttling the turbine. This requires making F_{load} equal to the resistive forces F_{visc}.

$$F_{load} = F_{visc} \tag{21}$$

Since $F_{conv} > 0$, and combining Equations (20) and (21) yields:

$$F_{load} = F_{visc} = \frac{F_{conv}}{2} > 0 \tag{22}$$

Therefore, for a given convection flow velocity v_{Flow}, the maximum power transferred to the turbine is:

$$P_{load} = F_{load} v_{Flow} = \frac{F_{conv} v_{Flow}}{2} \tag{23}$$

5. The Magnetostrictive Cycle-Source of Energy Driving Magnetic Convection

The following is a detailed description of the magnetostrictive cycle which explains that the energy driving magnetic convection originates from the thermal energy of the fluid. **Figure 2(a)** illustrates the engine's thermodynamic cycle as a rectangular pV diagram, each stage conducted either at constant pressures or at constant volume. The constant pressure stages of the cycle require that the hydrostatic pressure of both columns be equal at their bottoms and be equal at their tops. To account for the difference in density between the two columns, the right one is made slightly taller than the left one as shown in **Figure 2(b)**.

Let us open the loop in **Figure 1** by disconnecting the columns at the top and exposing them to the atmosphere, thereby allowing each column to reach its own equilibrium fluid level in accordance with hydrostatic principles. Obviously, in this open configuration, convection is not possible. However, *since the fluid in the magnetized column is less dense, hydrostatic equilibrium requires that its level be higher than in the other column* as shown in **Figure 2(b)**.

The difference in height of the fluid level is called a pressure head and is a function of the different densities in the columns. Since hydrostatic equilibrium requires that:

$$\rho g h = (\rho + \Delta\rho) g (h + \Delta h) \tag{24}$$

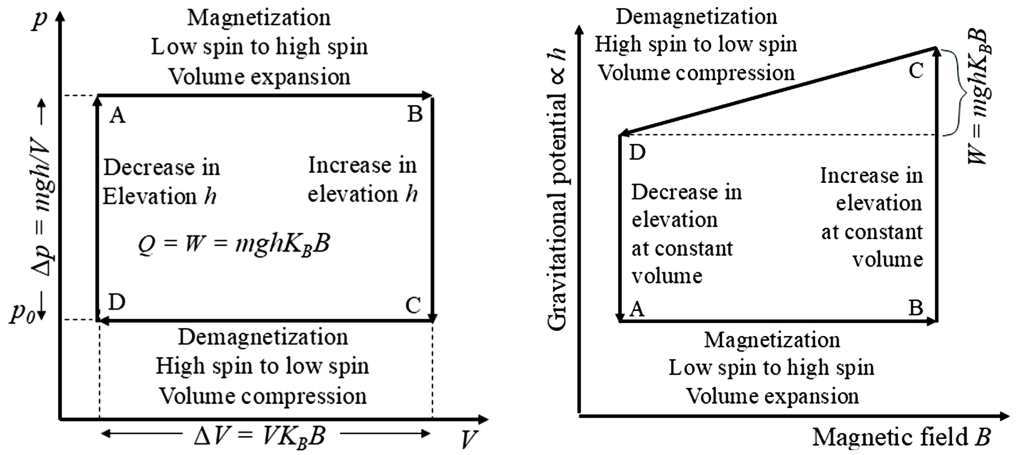

Figure 2. (a) Pressure-volume diagram of the magnetostricitive cycle. The fluid is assumed to be sterero-magnetostrictive and to change volume in a magnetic field, but to be incompressible under hydrostatic pressure. Accordingly, this cycle comprises two constant pressure stages and two constant volume stages. (b) To maintain equal hydrostatic pressures between the tops of each column, and also between the bottoms of each column, the column with the least dense fluid is made taller than the other one. Changes in magnetic energy cancel out and are not shown in the drawing.

Therefore, the pressure head is:

$$\Delta h \approx -\frac{\Delta\rho}{\rho} h \tag{25}$$

Combining Equations (1) and (25) yields:

$$\Delta h \approx K_m B h \tag{26}$$

Now, let us install a mini-turbine above the transition zone in the demagnetized region between the tops of the two columns, and configure it to extract energy from the fluid flowing from the high level to the low level. Let us adjust the throttle of the turbine to use up half the open circuit pressure head, leaving the other half to be absorbed by the viscous and dissipative processes around the loop. This is equivalent to optimal source-load matching in an electrical circuit.

The flow depletes the fluid at the higher level and produces an excess of fluid at the lower level, thereby breaking hydrostatic equilibrium. *The necessity to restore this equilibrium causes fluid to flow around the bottom of the loop to readjust the levels at the top, ultimately resulting in continuous convection.*

The following discussion is a detailed description of a four-stage thermodynamic cycle illustrated in **Figure 2** that accounts for all energy transfers. Stages AB and CD occur at constant pressure and include energy transfer terms that cancel out. Therefore, to simplify the math, these two stages shall be discussed together. Similarly, stages BC and DA occur at constant volume and shall be discussed together.

Stage AB: The fluid at the bottom of the loop flows from the demagnetized column into the magnetized column. The following happens:

1) Since the change in the magnetic field is $\Delta B = +B$, the fluid acquires internal

magnetic energy $(\mu_{magn}B)_{AB}$ where μ_{magn} is the magnetic moment.

2) Due to magnetostriction, the fluid expands by $\Delta V = VK_mB$ in proportion with its volume V, the magnetostrictive coefficient K_m and the field B.

3) Assuming an atmospheric pressure p_0, and a hydrostatic pressure $\Delta p = \rho gh$ at the bottom due to the height of the column, then the work performed on the surroundings due to the volume change is $W = (p_0 + \Delta p)\Delta V$ where $\Delta V = VK_mB$.

4) The process is endothermic and draws heat Q_{AB} from the surrounding:

$$Q_{AB} = \left(p_0 + \Delta p\right)\Delta V + \left(\mu_{magn}B\right)_{AB} \tag{27}$$

Stage CD: The fluid at the top flows from the magnetized column through the turbine into the demagnetized column. The following happens:

1) The change in the magnetic field is $\Delta B = -B$. Therefore, the fluid loses internal magnetic energy $(\mu_{magn}B)_{CD}$. Since the fluid is back to its initial magnetic state, $(\mu_{magn}B)_{AB} + (\mu_{magn}B)_{CD} = 0$.

2) Due to reverse magnetostriction, the fluid contracts by $-\Delta V = -VK_mB$.

3) Since the fluid is at atmospheric pressure, the work done by the fluid on the surroundings due to the volume change is $-p_0\Delta V$.

4) Therefore, the process is exothermic, and the transferred heat is:

$$Q_{CD} = -p_0\Delta V + \left(\mu_{magn}B\right)_{CD} \tag{28}$$

5) Now, let us combine Equations (27) and (28) in stages AB and CD. Since the molecules return to their original states and the magnetic potential is conservative, *i.e.*, $(\mu_{magn}B)_{AB} + (\mu_{msgn}B)_{CD} = 0$, all magnetic terms cancel out and the total heat transferred is:

$$\Delta Q = \Delta p\Delta V \tag{29}$$

Referring to Equation (29), the pressure difference Δp between the top and bottom of the columns is proportional to the height h of the column, *i.e.*, $\Delta p = \rho gh$. The change in volume ΔV due to magnetostriction is proportional to the change in height Δh, *i.e.*, $\Delta V/V = \Delta h/h$. And the mass of fluid m is $m = \rho V$. Plugging this information in Equation (29) yields:

$$\Delta Q = mg\Delta h \tag{30}$$

The other two stages, BC and DA, occur at constant volume and constant magnetic field. The only variable is the gravitational potential energy E of the fluid.

Stage BC: A mass m of fluid in the vertical magnetized columns BC experiences an increase in gravitational energy E as it moves up the magnetized column. Since the height of the columns is $h + \Delta h$ the change in potential energy is:

$$E_{BC} = mg\left(h + \Delta h\right) \tag{31}$$

Stage DA: The descending fluid in this demagnetized column experiences a drop in potential energy. Since the height of the columns is h the change in potential energy is:

$$E_{DA} = -mgh \tag{32}$$

The net change in potential energy for BC and DA is obtained by combining

Equations (31) and (32):

$$\Delta E = mg\Delta h \tag{33}$$

Comparing Equations (30) and (33) shows that the net input heat ΔQ is converted to a net potential energy increase ΔE of the fluid: $\Delta Q = \Delta E = mg\Delta h$. This is exactly the energy associated with the pressure head used by the turbine. Hence, the maximum work W that can be produced by the turbine (not accounting for viscous losses) is:

$$W = \Delta Q = \Delta E = mg\Delta h \tag{34}$$

Work can now be expressed as a function of design parameters B and h. From Equation (26) $\Delta h = K_m Bh$. Therefore

$$W = \Delta Q = \Delta E = mghK_B B \tag{35}$$

and since the fluid is back to its starting point after a cycle, the decrease in entropy experienced *by the surroundings* is:

$$\Delta S = -\frac{mghK_m B}{T} \tag{36}$$

Remarkably, this thought experiment concludes that a magnetic field and gravity are sufficient to drive isothermal convection without a temperature gradient or the need for a heat sink. Being static, these fields do not contribute any *net energy* to the process. They enable the process only by operating as "facilitators". This result is surprising but in-line with directives issued by Onsager who specifically excluded magnetic fields and rotation from reciprocals [47] [48].

6. Framework of Applicability of Second Law

How can magnetostrictive convection be possible given our conventional understanding of thermodynamics? To resolve this paradox, one must go back to foundational assumptions that clearly delineate the framework of applicability of the second law. The law is not universal. It is supported by evidence of two kinds, each having its own limitations:

1) Theoretical evidence and limitations.
2) Experimental evidence and limitations.

6.1. Theoretical Evidence and Limitations

Time-reversal symmetry, expressed at the microscale, occupies a special place in thermodynamics. It is a necessary condition for reversible processes such as the Carnot cycle [49]. *It is assumed in all proofs of the H-theorems* by their authors:

- Boltzmann uses his time symmetric equation in which the collision term satisfies detailed balance: the rate of collisions A + B → C + D equals the rate of C + D → A + B in equilibrium [50]-[52].
- Tolman explicitly states that collisions are "unbiased"—meaning microscopic reversibility holds [53].
- Gibbs uses the Liouville equation which preserves phase space volume precisely

because the underlying Hamiltonian dynamics are time-reversal symmetric [54].

- von Neumann relies on unitary evolution under time-symmetric Hamiltonians as expressed in the early symmetric formulation of quantum mechanics, not the newer QED and QCD versions which have been extended to include CPT electromagnetic symmetry [55] [56].

Time-reversal symmetry guarantees that equilibrium can be reached in a state of maximum entropy. It is postulated by Lars Onsager [47] [48] when he excludes time asymmetric phenomena (the magnetic field and rotation) from his reciprocals. It is required in the fluctuation theorem by Evans, Cohen and Morriss [57], Evans, and Searles [58] [59] and Crooks [60], in which fluctuations are assumed to be time symmetric.

In contrast, we are familiar with large scale time-reversal asymmetry, *i.e.*, the irreversibility of the macro-world. It is due to "coarse graining", *i.e.*, the loss of information which occurs when the description of a system shifts from microstates to macrostates.

This paper focuses, not on the large-scale asymmetry of the macro-world, but on the assumption of time-reversal symmetry of the H-theorem and the theoretical limits this assumption imposes on the coverage of the second law.

Notwithstanding the H-theorem, nature is not exclusively time-reversal symmetric. For example, the electromagnetic field is charge, parity time (CPT) symmetric as evidenced by the right-hand rule. See **Appendix 3** (Clarification of time-reversal asymmetry).

As shown by Levy [61]-[66], time-reversal asymmetry as produced by the magnetic field can result in extraordinary thermodynamic effects: Combined with the electric field, it produces the $E \times B$ thermoelectric effect that converts heat to electrical energy, isothermally, with no need for separate heat source and heat sink. See **Appendix 4** (The $E \times B$ thermoelectric effect).

In summary, there is no theoretical reason that forbids magnetostrictive convection. This phenomenon falls outside the coverage of the second law.

6.2. Experimental Evidence and Limitations

Countless experiments have been performed to test the second law. Many did include magnetic fields. However, to the best of my knowledge, no experiment has been conducted which combines magnetostrictive materials, the magnetic field and gravity, and with the specific purpose of inducing convection. Therefore, there is no experimental evidence against magnetostrictive convection.

In addition, recent groundbreaking experiments raise interesting questions on the isothermal conversion of heat, further shaking the foundations of thermodynamics:

Lee [67]-[69] reports the existence of anaerobic microorganisms capable of utilizing heat energy isothermally to produce ATP without the existence of a temperature gradient. His experiments with Methanosarcina, show that the isothermal con-

version of heat to ATP by these organisms causes a drop in the temperature of the liquid culture by as much as 0.45˚C with a mean drop of 0.25˚C ± 0.06˚C. Lee calls the metabolic mechanisms used by these micro-organisms, type-B processes to differentiate them from classical processes such as heat engines, which he calls type-A processes.

Sheehan *et al.* [70] [71] report an anisotropic diffusion through a chemically asymmetric membrane, which causes a difference in concentration across the membrane. This concentration difference then drives a concentration cell that produces electrical energy with a power density that might exceed 10^7 Watts/m^3.

Furthermore, Sheehan *et al.* also experiment [72] with epicatalytic asymmetric filaments of rhenium and tungsten in a molecular hydrogen. The asymmetric chemical reactions at the surface of the two filaments produce a temperature difference of more than 120 K.

Nikulov [73] and Gurtovoi *et al.* [74] observe a DC voltage on an asymmetric microscopic superconducting ring when the ring or its segments are switched between superconducting and normal state by non-equilibrium noises. This voltage indicates that one of the ring segments operates as a dc power source.

Fu and Fu [75] describe an experiment in which a magnetic field directs thermally emitted electrons from a first Ag-O-Cs plate to a second identical plate in a vacuum tube, thereby causing an isothermal potential difference and current between the plates.

Kondo *et al.* [76] develop a new organic thermoelectric device, capable of functioning at room temperature without a temperature gradient. The key finding in their research was compounds that work well as charge transfer interfaces, in other words, that can easily transfer electrons between each other. Their device produces an open-circuit voltage of 384 mV, a short-circuit current density of 1.1 μA/cm^2, and maximum output Pmax of 94 nW/cm^2.

In summary, the law is not violated, it is bypassed. It remains valid within its domain of applicability (time-reversal symmetric processes), but does not include magnetostrictive systems.

7. Proposed Experiment for Testing Magnetostrictive Convection

In the experiment described below a magnetostrictive fluid is used to test whether magnetostrictive convection is possible. In principle, however, a solid Joule magnetostrictive material may also be used, see **Appendix 5** (Isothermal engine using solid joule magnetostriction).

The discussion includes the selection of materials and the fabrication and test of a device.

7.1. Material Selection

The working fluid comprises a solvent holding stereo-magnetostrictive molecules that change volume when exposed to a magnetic field. This rules out many mate-

rials such as:

- Ferromagnetic liquids which include magnetic particles in a solvent that respond to a magnetic field by reorienting themselves, not by changing their shape or volume.
- Suspensions in liquids of Joule magnetostrictive materials such as Gerfenol-D, Terfenol-D, nickel, iron-gallium (Galfenol), which change shape but not volume.

This requirement qualifies Fe(II) and Fe(III) complexes in which spin cross-over produces a volume change.

1) Particles should be as small as possible to overcome magnetic forces F_{magn} caused by field non-uniformity. These forces are proportional to the magnetic moment μ_{magn} of the particles, and the field gradient ∇B, *i.e.*, $F_{magn} \propto \mu_{magn} B$.

2) Surfactants should be added to avoid settling caused by gravity.

3) Operation should be at room temperature (300 K) to avoid the need for external heating or cooling and to exploit ambient heat.

4) Performance can be optimized by operating at the edge of chaos or at the thermodynamic threshold, an optimization technique described in Section 8 and applied by Levy to optimize the $E \times B$ thermoelectric effect. In the context of the magnetostrictive engine, this means operating at the transition temperature of the magnetostrictive material. This is the point where the smallest magnetic field produces the largest magnetic strain index $K_m = (\Delta V/V)/B$ and occurs near the inflection point of the distribution. See Note 2) and Section 8.

5) The solvent should have a low viscosity. Acetone is an attractive solvent with low viscosity, but from an implementation point of view, water is better.

Tables 2(a)-(c) list several stereo-magnetostrictive materials and their properties which best fit the requirements set forth above. The tables show that stereo-magnetostrictive materials are relatively incompressible under gravitational pressure but change their volume significantly in a magnetic field (as assumed in the thought experiment.) See Notes 5) and 6).

In the experiment discussed in this paper, the term $K_p p$ is negligible compared to $K_m B$. Using the values in Table 2(a), we find that:

- For $B = 1$ Tesla, $K_m B = 5 \times 10^{-3}$,
- For $p = 2000$ Pa (20 cm of water as described in the experiment) $K_p p = 8 \times 10^{-8}$.

Accordingly, the change in volume ratio due to the magnetic field is six orders of magnitude larger than the one due to pressure. Therefore, the approximation made in the thought experiment, that the liquid is incompressible under gravity, is justified.

To further maximize the effect of the magnetic field on volume, it is important to operate at or near the HS/LS transition temperature. Room temperature is ideal to fully use ambient heat "as is", and avoid having to heat or cool the experiment. Selecting material for this transition temperature requirement is challenging as these materials behave differently—have different transition temperatures—when they are in solution (Notes 2) and 3)) and when they are exposed to a field. The

properties listed in Tables 2(a)-(c) are best estimates based on current literature but need to be verified experimentally for particular solvents and field intensities. Given this caveat, $Fe(NH_2trz)_{32}$ might be the best option among the above materials because:

1) It has one of the highest sensitivities to magnetic fields.
2) It is relatively stable in solution.
3) Its synthesis is well-documented.

Table 2. (a) Properties of $Fe(NH_2trz)_{32}$ or $\left[Fe\left(NH_2trz\right)_3\right]^{2+}\left(NO_3^-\right)_2$ (Iron coordinated to three amino-triazole ligands, with two nitrate counter-ions); (b) Properties of $[Fe(bpz)_2(phen)]$ (Iron coordinated to two bis(pyrazol-1-yl) and one phenanthroline ligands); (c) Properties of $[Fe(phen)_2(NCS)_2]$ (Iron coordinated to two phenanthroline ligands and two thiocyanate ligands).

(a)

Transition temperature (K)	295 - 305	Kröber *et al.*, 1994 [7]
Width of transition region (K)	10 - 15	Roubeau, 2012 [8]
$K_m = (\Delta V/V)/\Delta B$ (T^{-1})	$1 - 5 \times 10^{-4}$	Rotaru *et al.*, 2013 [9]; Grosjean *et al.*, 2013 [13]
$K_p = (\Delta V/V)/\Delta p$ (Pa^{-1})	-4×10^{-11}	Ksenofontov *et al.*, 2004 [10]
Saturation mag. field B_{Sat} (T)	~0.5 - 1.0	Bousseksou *et al.*, 2011 [11]; Rotaru, 2013 [9]
Hysteresis relaxation time (μsec)	~10 - 100	Gutlich *et al.*, 2013 [29]; Nicolazzi, 2018 [38]
Max volume ratio change	$\sim 6 - 8 \times 10^{-2}$	Guionneau *et al.*, 2004 [12]
Hysteresis (Tesla wide)	0.3 - 0.4	Rotaru *et al.*, 2013 [9]; N/A, see Note 2)
Density (gm/cm^3)	1.8	Grosjean *et al.*, 2013 [13]

(b)

Transition temperature (K)	285 - 290	Real *et al.*, 2003 [14]
Width of transition region (K)	20 - 25	Galet *et al.*, 2006 [15]
$K_m = (\Delta V/V)/\Delta B$ (T^{-1})	$0.8 - 3 \times 10^{-4}$	Halcrow, 2011 [16]; Real *et al.*, 2003 [14]
$K_p = (\Delta V/V)/\Delta p$ (per 100 MPa)	$\sim -3 \times 10^{-11}$	Ksenofontov *et al.*, 2004 [10]
Saturation mag. field B_{Sat} (Tesla)	~0.3 - 0.8	Bonhommeau *et al.*, 2006 [17]; Bousseksou *et al.*, 2005 [18]
Hysteresis relaxation time (μsec)	~50 - 200	Halcrow, 2013 [19]; Gutlich *et al.*, 2013 [29]
Max vol change ratio	$\sim 4 - 5 \times 10^{-2}$	Real *et al.*, 2003 [14]
Hysteresis (Tesla wide)	<0.1	Bousseksou *et al.*, 2005 [18]; N/A, see Note 2)
Density (gm/cm^3)	1.6 - 1.7	Halcrow, 2013 [19]

(c)

Transition temperature (K)	176 - 180	König, E., 1991 [20]; Boillot *et al.* 1999 [23]
Width of transition region (K)	5 - 8	Bau, R., 1981 [21]
$K_m = (\Delta V/V)/\Delta B$ (per Tesla)	$0.5 - 2 \times 10^{-4}$	Bousseksou *et al.*, 2000 [22]; Gütlich *et al.*, 2004 [27]
$K_p = (\Delta V/V)/\Delta p$ (per 100 MPa)	-3.5×10^{-11}	Ksenofontov *et al.*, 2004 [10]; Gütlich *et al.*, 2004 [27]
Saturation mag. field B_{Sat} (T)	~0.2 - 0.6	Bousseksou *et al.*, 2011 [11] ; Gütlich, 2004 [27]
Hysteresis relaxation time (μsec)	20 - 80	Sorai & Seki, 1974 [25]; Gütlich *et al.*, 2004, [27]
Max vol change ratio	$\sim 3 - 5 \times 10^{-2}$	Guionneau *et al.*, 2004 [12]
Hysteresis (Tesla wide)	~0.2 - 0.3	Boillot *et al.*, 2004 [23]; N/A, see Note 2)
Density (gm/cm^3)	1.4 - 1.5	Varret *et al.*, 2002 [24]

7.2. Convection Engine Using Fluid Stereo-Magnetostriction

Figure 3 is a physical implementation of the magnetostrictive engine shown in Figure 1.

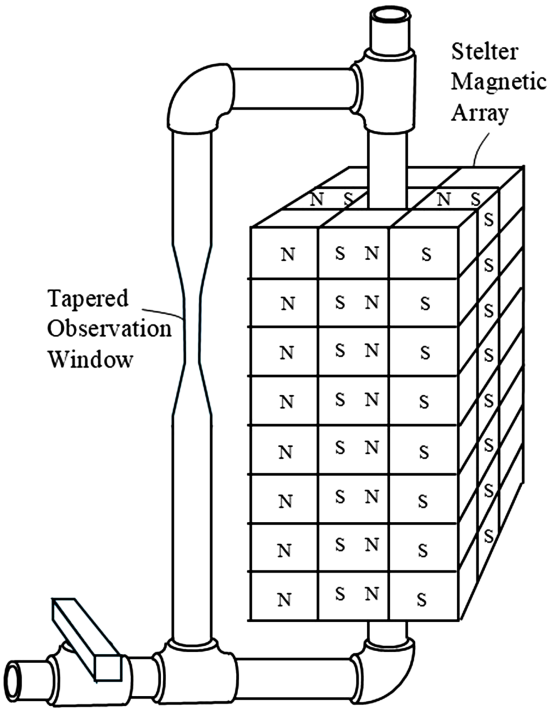

Figure 3. Experimental device. A fluid comprising stereo-magnetostrictive molecules can convect in a closed tube looping around a stack of Stelter magnets. Convection can easily be observed by using a transparent tube, adding glitter to the fluid, and tapering a portion of the tube to accelerate the flow. The figure shows a 20 cm stack of 8 layers, each layer comprised of eight 2.5 cm cubic magnets. A 16-layer stack of 1.25 cm magnets may also be used and be more practical.

The magnetic field is produced by a stack of Stelter arrays, each array consisting of 8 N52 Neodymium magnets arranged in a square formation with an empty space in its center. Each Stelter array operates as a rough approximation of a circular Halbach array but is much simpler to implement because it only requires cubic magnets, not arc magnets. The stacked arrays form a vertical cavity that holds a horizontal and uniform magnetic field.

The remanence of a N52 magnet is approximately 1.45 - 1.48 Teslas. Furthermore, the intensity of the magnetic field inside a Stelter array increases in proportion to ln(OP/IP) where OP is the outer perimeter and IP is the inside perimeter of the array [77] [78]. Therefore, for an array comprised of cubic magnets ln(OP/IP) = ln(3) = 1.09, the magnetic field inside an array of N52 magnets is about 1.58 - 1.61 T. (Similarly, N42 magnets would produce a field of 1.42 - 1.44 Tesla).

The magnetostrictive engine also includes a flexible tube which contains the stereo-magnetostrictive fluid comprised of stereo-magnetostrictive particles sus-

pended in a solvent. The tube loops through and around this vertical cavity in which the fluid is exposed to the magnetic field. Let n be the volume fraction of magnetostrictive particles, and $1 - n$ be the volume fraction of the solvent. Let the stereomagnetostrictive index of the fluid plus particles be symbolized by K_{mFluid}, and that of the particles only by $K_{mParticles}$. From Equation (1), the strain of the fluid can then be expressed as a fraction of the strain of the particles:

$$s_{Fluid} = K_{mFluid} B = \left(\frac{\Delta V}{V}\right)_{Fluid} = n\left(\frac{\Delta V}{V}\right)_{Particles} = nK_{mParticles} B \tag{37}$$

The level difference between the columns is given by Equation (26) as illustrated in **Figure 2(b)**. Scaling it in accordance with Equation (37) to include the volume fraction yields:

$$\Delta h = nK_{mParticles} Bh \tag{38}$$

The dynamic range of the magnetic field should be within saturation, *i.e.*, $B < B_{Sat}$. (see Note 4)) and **Tables 2(a)-(c)**. The pressure head Δh corresponds to a pressure:

$$p_{conv} = \rho g \Delta h = \left(\rho g n K_{mParticles} B\right) h \tag{39}$$

The parentheses have been added to this equation to emphasize that p_{conv} can be made arbitrarily large by increasing h. Any *fixed* back pressure caused by transition point effects can be overcome by increasing h.

The volumetric flow rate of the fluid around the loop can now be calculated. Assuming a fluid viscosity η, a pressure difference p_{conv}, a tube of radius r, and length L, Poiseuille's Law yields:

$$Q_{Flow} = \left(\frac{\pi p_h}{8\eta L}\right) r^4 \tag{40}$$

Parentheses have been inserted to emphasize that for a given fluid viscosity η and head pressure p_{conv}, the flow can be increased by increasing the radius r of the tube.

The average flow velocity is obtained by dividing Q_{Flow} by the cross-sectional area πr^2:

$$v_{Flow} = \frac{Q_{Flow}}{\pi r^2} = \frac{p_{conv}}{8\eta L}\left(r^2\right) \tag{41}$$

Substituting the pressure p_{conv} from Equation (39) into Equation (41) gives the convective flow velocity as a function of the field and of the magnetostriction index:

$$v_{Flow} = \left(\frac{\rho g h n K_{mParticles} B}{8\eta L}\right) r^2 \tag{42}$$

Note that since the length L of the loop is about equal to twice its height h, *i.e.*, $h/L \approx 1/2$ Equation (42) can be written as:

$$v_{Flow} = \left(\frac{\rho g n K_{mParticles} B}{16\eta}\right) r^2 \tag{43}$$

which indicates that a taller loop raises the pressure head but also raises viscous length; they cancel. Therefore, velocity is not a function of h but of the radius r of the tube: even though increasing height does increase the convective drive due to the head pressure p_{conv}, it also increases frictional losses along the tube. Overall, these two effects cancel each other out. Equation (43) also shows that one can overcome viscous forces by increasing the radius of the tube.

Combining Equations (39) and (40) and using $h/L \approx 1/2$ gives the power output $P = p_{conv}Q_{Flow}$:

$$P = p_{conv}Q_{Flow} = \left[\frac{\pi\left(\rho g n K_{mParticles} B\right)^2}{16\eta}\right] hr^4 \tag{44}$$

and the power per unit area is:

$$\frac{P}{\pi r^2} = \left[\frac{\left(\rho g n K_{mParticles} B\right)^2}{16\eta}\right] hr^2 \tag{45}$$

As an example, let us consider an experimental device with the following parameters selected for the least expensive design, yet produce observable results:

- Fluid: $Fe(NH_2trz)_{32}$ particles suspended in water-chosen because it has the highest K_m (stereo-magnetostrictive volume ratio modulus), as shown in **Tables 2(a)-(c)**.
- $r = 0.005$ m (assume a 1 cm ID cylindrical tubing).
- $h = 0.2$ m.
- $L = 2h$ (total length L of the loop is equal to twice the height h of the loop).
- $n = 0.1$ (keep the volume ratio of particles to solvent low enough to ensure low viscosity).
- $\rho = 1000$ kg/m^3 (assume an aqueous solvent).
- $K_{mParticles} = 0.0003$ Tesla^{-1} (From **Table 2(a)**, strain by one Tesla for the stereo-magnetostrictive fluid $Fe(NH_2trz)_{32}$).
- $\eta = 0.001$ N·s/m^2 (viscosity of water at 20 C).
- $B = 0.8$T (approximately the maximum field produced by a Stelter array of N52 magnets) comparable to the saturation field $B_{Sat} \approx 0.5$ - 1.0 Tesla (**Table 2(a)**, [77]).

Using the above quantities the following can be calculated:

- $A = 78.5$ mm^2.
- $\Delta h = 4.8$ μ pressure head.
- $p_{conv} = 0.048$ N/m^2.
- $Q_{Flow} = 29.4 \times 10^{-9}$ m^3/s.
- $v_{Flow} = 0.375$ mm/sec.
- $P = 1.41 \times 10^{-6}$ mW.
- $P/A = 1.8 \times 10^{-6}$ mW/cm^2.
- $P_{Load} = 0.705 \times 10^{-6}$ mW (Maximum power available to matched load is $1/2P$).

The resulting convective flow velocity $v_{Flow} = 0.375$mm/sec, is small but observable. The tube can be tapered as shown in **Figure 3** to reduce its inner diameter

locally from 1cm to 0.6cm. This would accelerate the flow by a factor of 2.8 making the flow an easily observable 1 mm/sec. Observing this flow can be facilitated by adding some glitter particles or fluorescent molecules to the solution or by means of a sensitive flowmeter.

Increasing the dimensions of the device by a factor of 100 (*i.e.*, $h = 20$ m, $r = 0.5$ m) increases the flow velocity by 10,000 to 3.75 m/s and the power by a factor of 10^{10} to 14.1 W.

8. Operating at the Thermodynamic Threshold to Maximize Performance

The power generated in the above experiment is minuscule. However, the goal of this paper is not to uncover any specific large source of power but *to clearly expose a shortcoming of thermodynamics as currently understood*: *the second law is not universal but is limited to time-reversal symmetric phenomena*. This section discusses a methodology for maximizing power output.

Phenomena capable of isothermal thermal conversion do not occur in isolation. Two kinds of processes occur concurrently:

1) Time-reversal asymmetric processes that fall outside the coverage of the second law.

2) Time symmetric processes (the ones mentioned in the H-theorem) which occur in the background.

In carelessly designed experiments, symmetric processes always dominate and mask out the much weaker asymmetric ones. These experiments fail, not because of the second law, but because their anomalous behavior is too small to be measured. To avoid this outcome, one must amplify the expression of their asymmetry. This can be done by running the experiment at the thermodynamic threshold, a method that has successfully been applied to the $E \times B$ thermoelectric effect (see **Appendix 4**) and which leverages on the basic assumption of the H-theorem, that all phenomena are *time-reversal symmetric at the microscopic scale* [50] [56]. This approach requires quantifying the concepts of "*time asymmetry*" and "*microscopic scale*" and involves four steps:

1) Defining a model of the phenomenon.

2) Identifying a characteristic measure of the background *symmetrical thermal processes* operating at the microscopic scale, in given units.

3) Identifying a characteristic measure of the *time-reversal asymmetry* expressed in the same units.

4) Equating these two measures to produce an optimal design that operates at the thermodynamic threshold.

8.1. Model of Magnetic Convection

The magnetostrictive effect is due to a step in the spin energy ΔE_S that changes the volume ΔV. For a given pressure p, the magnetostrictive energy equation is:

$$E_M = \Delta E_S + p\Delta V \tag{46}$$

The change in the volume ratio $\Delta V/V$ due to ΔB is equal to $K_m \Delta B$ where K_m is the magnetostrictive modulus for the bulk volume ratio. Similarly, the change in $\Delta V/V$ due to Δp is $K_P \Delta p$ where K_P is the pressure modulus for the bulk volume ratio. Hence, the total change in volume ratio due to changes in magnetic field and pressure is:

$$\text{Change in volume ratio} = \frac{\Delta V}{V} = K_p \Delta p - K_m \Delta B \tag{47}$$

A molecule of mass m of a material of density ρ has a volume $V = m/\rho$. Therefore, combining Equations (46) and (47) yields for a molecule:

$$E_M = \Delta E_S + P\frac{m}{\rho}\left(K_p \Delta p - K_m \Delta B\right) \tag{48}$$

In the presence of degeneracy g_{HS} and g_{LS} in spin states, the Fermi-Dirac distribution can be expressed with g_{HS} and g_{LS} outside the exponent as [44]:

$$n_{HS} = \frac{g_{HS}}{g_{HS} + g_{LS} \exp\left[\left(E-\mu\right)/k_B T\right]} \tag{49}$$

or as an energy term inside the exponent:

$$n_{HS} = \frac{1}{1+\exp\left[\dfrac{E-\mu-k_B T \ln\left(g_{HS}/g_{LS}\right)}{k_B T}\right]} \tag{50}$$

Correcting Equation (48) to express the degeneracy as an energy yields

$$E_M = \Delta E_S + P\frac{m}{\rho}\left(K_p \Delta p - K_m \Delta B\right) + k_B T \ln\left(g_{LS}/g_{HS}\right) \tag{51}$$

and the corresponding Fermi-Dirac occupancy distribution of the HS states becomes:

$$n_{HS} = \frac{1}{1+\exp\left(\dfrac{E-E_M}{k_B T}\right)} \tag{52}$$

8.2. Identifying the Measure of the Background Symmetrical Thermal Processes

The thermal energy $k_B T$ represents the symmetry measure.

$$\text{Measure of symmetry} = k_B T \tag{53}$$

8.3. Identifying the Measure of the Time-Reversal Asymmetry

In the magnetostrictive convection engine, the change in energy E_M described by Equation (51) between HS and LS states represents the asymmetry measure and is due to the magnetic field that causes a shift in the distribution of the states.

8.4. Equating Measures for the Thermodynamic Threshold

The magnetic field can skew the spin occupancy distribution with respect to the origin, as shown in **Figure 4**.

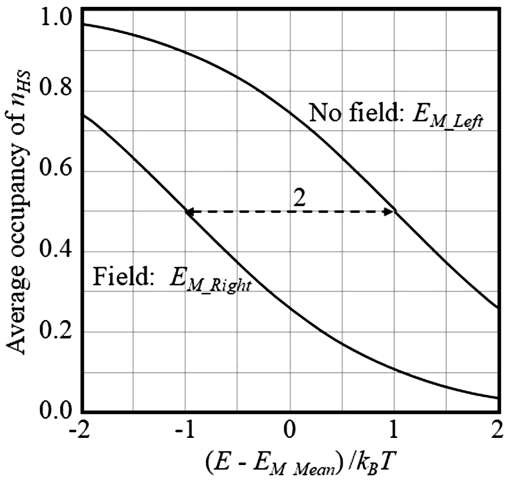

Figure 4. Distribution functions for left and right sides. The magnetic field on the right of the device causes a shift to the left of the distribution, equal to k_BT, and the absence of field on the left, a symmetrical shift to the right.

Decreasing the field shifts the distribution left. Increasing the field shifts it to the right. On the left side of the convection device $B = 0$. Therefore, from Equation (51) E_{M_Left} is:

$$E_{M\_Left} = \Delta E_S + p\frac{m}{\rho}\left(K_p \Delta p\right) + k_B T \ln\left(g_{LS}/g_{HS}\right) \tag{54}$$

and on the right side of the device, where B is non-zero, E_{M_Right} is:

$$E_{M\_Right} = \Delta E_S + p\frac{m}{\rho}\left(K_p \Delta p - K_m B\right) + k_B T \ln\left(g_{LS}/g_{HS}\right) \tag{55}$$

Combining Equations (54) and (55) yields:

$$E_{M\_Left} - E_{M\_Right} = p\frac{m}{\rho}K_m B \tag{56}$$

Defining the mean energy as:

$$E_{M\_Mean} = \frac{E_{M\_Left} + E_{M\_Right}}{2} \tag{57}$$

the measure of asymmetry can be taken as the distance between E_{M_Left} and E_{M_Right} and their mean:

$$\begin{aligned} &\text{Measure of asymmetry} = E_{M\_Left} - E_{M\_Mean} \\ &= E_{M\_Mean} - E_{M\_Right} = \frac{E_{M\_Left} - E_{M\_Right}}{2} \end{aligned} \tag{58}$$

which in combination with Equation (56) yields

$$\text{Measure of asymmetry} = p\frac{m}{2\rho}K_m B \tag{59}$$

In accordance with the thermodynamic threshold optimization method, equating the measure of asymmetry in Equation (59) with the measure of symmetry in Equation (53) yields:

$$E_{M\_Left} - \frac{E_{M\_Left} - E_{M\_Right}}{2} = k_B T \tag{60}$$

Now, combining Equations (56) and (60) yields the optimum magnetic field as a function of temperature and pressure:

$$B = \left(\frac{2k_B \rho}{K_m m}\right)\frac{T}{p} \tag{61}$$

As shown in **Figure 4**, the Fermi-Dirac occupancy distribution of the high spin states n_{HS} of Equation (52) is plotted for E_{M_Left} and E_{M_Right} as a function of the scaled value $(E - E_{M\_Mean})/k_B T$.

Equation (61) provides optimal design parameters. Selecting a lower field value than the one in this equation would allow the LS states to dominate around the loop and no convection would occur.

A higher value of B would allow the HS states to dominate in the magnetized portion of the loop and convection would take place, but not in the most efficient manner. For example, increasing the density of the fluid, increasing the temperature, or decreasing the pressure would result in a higher output.

Even though Equation (61) provides design guidelines, it should be used only in the context of a constrained optimization approach that takes into account the range of applicability of the model, the availability of materials with desired properties and the limitations in intensity of the magnetic field and gravity. Because of these real-life constraints, the power transmitted to a load by the device in this experiment is only 0.705×10^{-6} mW.

In contrast, other techniques are not so limited. For example, in the $E \times B$ thermoelectric effect described by Levy [61]-[66], gravity is replaced by the much stronger electric field, and spin cross over molecules, by highly mobile electrical carriers. This effect can produce up to 136 mW/mm^2 or 400 times more energy than the Shockley-Queisser solar cell limit [79] [80].

9. Suggested Extension of Second Law and Entropy to Include Symmetry-Breaking Phenomena

Symmetry implies redundancy of information: fewer bits are needed to describe a system. Conversely, symmetry-breaking eliminates this redundancy and requires more bits. In a conventional thermodynamics reversible process, forward and reverse behaviors are identical because the process is assumed to be time-reversal symmetric as assumed in the H-theorem. Therefore, the entropy of a system sufficient to determine its forward behavior is also sufficient for reverse behavior and for making the system reversible.

However, certain physical phenomena break the time-reversal symmetry, thereby producing additional states such as spin and field orientations. These new states preclude equilibrium by enforcing a forward or reverse direction of a process as demonstrated by the $E \times B$ drift and magnetic convection. Accordingly, a complete formulation of entropy that accounts for all states should have two compo-

nents:

1) A classical entropy component S_A which encodes the information associated with time-reversal symmetric "A" processes. Being additive, it can represent multiple processes with a sum $S_A = \Sigma S_{Ai}$. As required by H-theorem, S_A cannot decrease:

$$\frac{\mathrm{d}S_A}{\mathrm{d}t} \geq 0 \tag{62}$$

2) An anomalous entropy components S_B which encodes the information of anomalous "B" processes that breaks time-reversal symmetry. It is also additive such that $S_B = \Sigma S_{Bi}$. S_B is not bound by the limitation of the H-theorem.

The net entropy S of a system would then be the sum:

$$S = S_A + S_B \tag{63}$$

10. Conclusions

A proof is presented as a thought experiment showing that a magnetic field can induce the convection of a magnetostrictive fluid in the absence of any temperature gradient. The energy driving this convection is drawn from the heat within the material. Forces that may retard convection can be either dissipative or conservative. Dissipative forces are flow-velocity dependent. They can slow down convection but cannot stop it. They can also be lessened by increasing the dimension of the system. Conservative forces do create a barrier to fluid flow, but this barrier has no net effect. The fluid acquires as much energy descending it as it loses climbing it.

This result justifies Onsager's warning that the magnetic field and rotation conflict with, and should be excluded from, his reciprocals. This conflict arises from the difference in the symmetries between conventional thermodynamics and magnetic phenomena. At the microscale, thermodynamics operates under the postulate of time-reversal symmetry: all processes behave identically when observed backward in time. This assumption, made in all H-theorems by Boltzmann [50]-[52], Tolman [53], Gibbs [54], and von Neumann [55] [56], is a necessary condition for reversible processes such as the Carnot cycle [49]. It ensures that systems adhere to equilibrium dynamics and preserve the fundamental laws governing entropy and energy.

However, the magnetic field is not time-reversal symmetric. It complies with Charge-Parity-Time (CPT) symmetry, a framework distinct from the time-reversal symmetry required by classical thermodynamics.

Falling outside the box defined by the H-theorem is not sufficient for a magnetic phenomenon to produce an *observable* anomalous thermoelectric effect. Without proper precautions, the large symmetric processes occurring in the background dominate the much smaller asymmetric ones, making them unobservable. Thermodynamic threshold optimization provides design guidelines that resolve this issue. This method involves defining a measure of asymmetry and a measure of sym-

metry. Optimal performance is achieved when a system is designed to operate such that both measures are equal.

In the context of magnetostrictive convection, this criterion implies that the device should operate near the transition temperature of the material, where the electronic configuration switches most spontaneously between LS and HS.

The breaking of time-reversal symmetry by the magnetic field generates thermodynamic information not accounted for by conventional entropy. It is therefore suggested to add an anomalous component S_B to the classical term S_A to properly account for this additional information.

An experiment proposed for testing this theory is expected to produce an easily observable convection. Its flow speed increases markedly with the dimensions of the device. With a height of 0.2 m and a tube radius of 0.005 m, the speed is 0.375 mm/s, whereas with a height of 20 m and a radius of 0.5 m, it reaches 3.75 m/s. While the smaller experiment is economically feasible and the larger is not, because of magnet size and cost, the speed of convection is not at issue. The purpose of this experiment, whether performed in thought or in the lab, is to unambiguously show that the second law is not universal. It has limits and can be bypassed.

The magnetostrictive effect discussed in this paper induces convection by combining a magnetic field with gravity. In contrast, another related phenomenon, the $E \times B$ thermoelectric effect [61]-[66], replaces gravity with the much stronger electric field, and the spin cross over molecules with high mobility electrical carriers in a semiconductor. Levy [66] shows that a fully optimized $E \times B$ effect device, fabricated in a high mobility semiconductor, can produce 136 mW/mm^2 or 400 times more energy than the Shockley-Queisser solar cell limit [79] [80]. Given the high power of the $E \times B$ effect, why be concerned at all with magnetostrictive convection? Its appeal does not lie in its power output, but in its ability to convey clearly and simply the limitations of the second law as currently understood, and the benefits of using magnetic fields for thermoelectric conversion of heat to energy at ambient temperature.

Data Availability Statement

Please contact the author for additional information.

Acknowledgment

I thank the inquisitive, open-minded and courageous scientists who, in the words of Richard P. Feynman, are "never certain... We absolutely must leave room for doubt or there is no progress and there is no learning" [81].

I also thank my wife Penny for her unwavering support, and my children, grandchildren and all future generations of the world who motivate me to pursue this research for tikkun olam.

Notes

1) If a static and permanent force opposing F_{conv} did exist, switching the load to

a fully conductive state would produce a backward convective flow in violation either of 1) the first law or 2) the second law, without the justification embodied by magnetostrictive effect as proposed in this paper.

2) Sometimes, the spin cross-over process is cooperative, meaning the transition occurs abruptly over a narrow temperature range. This cooperativity may be desirable if operation is desired over a narrow temperature range.

a) Cross-over compounds in solution have properties significantly different than in solid state. For example, $[Fe(phen)_2(NCS)_2]$ in solution exhibits the following changes: transition temperature increases from ~176 - 180 K (solid) to ~280 - 290 K in solution, with the exact value depending on solvent choice and concentration [23].

b) Transition Width: Broadens from 5 - 8 K to 25 - 35 K due to reduced cooperative effects between molecules [21].

c) Maximum Volume Change: While the molecular-level volume change remains similar (3% - 5%), the observed bulk effect is diluted by the solvent, resulting in much smaller effective density changes (typically 0.5% - 1% of solid-state effect at 0.1M concentration) [12].

d) Field Sensitivity: $K_m = (\Delta V/V)/\Delta B$ is slightly reduced in solution but remains measurable with sensitive equipment.

3) The solution form offers superior reversibility, tunability and low hysteresis through solvent selection, but at the cost of a significantly reduced magnitude of observable effects.

4) Limitations due to spin state saturation and permanent magnets. Increasing the magnetic field can speed up convection but up to a point. Two kinds of limitations arise:

a) Spin state saturation. A large field may cause the cross-over spin state to saturate, causing the relationship $\Delta V/V = K_m B$ to become non-linear and the magnetostrictive volume ratio modulus K_m to decrease. The solution to this problem is not to increase the field beyond saturation. Doing so would be wasteful and ineffectual.

b) Availability of strong permanent magnets. Magnetic convection is much more appealing with static fields. However, permanent magnets are limited to a few Teslas.

5) K_m is a *local, temperature-dependent slope* $(\partial \ln V/\partial B)_T$ evaluated near $T_{1/2}$. Reported values assume operation within the thermal transition region; away from $T_{1/2}$ $K_m \to 0$.

6) For SCO solids, magnetic fields of a few tesla primarily *shift* $T_{1/2}$ (e.g., −0.11 K at 5 T for $Fe(phen)_2(NCS)_2$), rather than drive full conversion at fixed T. Values of $T_{1/2}$, ΔT and density *depend strongly on counter-anion and hydration*.

Conflicts of Interest

The author declares no conflicts of interest regarding the publication of this paper.

References

[1] Joule, J.P. (1847) XVII. On the Effects of Magnetism Upon the Dimensions of Iron

and Steel Bars. *The London, Edinburgh, and Dublin Philosophical Magazine and Journal of Science*, **30**, 76-87. https://doi.org/10.1080/14786444708645656

[2] Cullity, B.D. and Graham, C.D. (2011) Introduction to Magnetic Materials. 2nd Edition, Wiley-IEEE Press.

[3] Clark, A.E. (1980) Chapter 7 Magnetostrictive Rare Earth-Fe_2 Compounds. In: *Handbook of Ferromagnetic Materials*, Elsevier, 531-589. https://doi.org/10.1016/s1574-9304(05)80122-1

[4] Olabi, A.G. and Grunwald, A. (2008) Design and Application of Magnetostrictive Materials. *Materials & Design*, **29**, 469-483. https://doi.org/10.1016/j.matdes.2006.12.016

[5] Grössinger, R., Turtelli, R.S. and Mehmood, N. (2014) Materials with High Magnetostriction. *IOP Conference Series: Materials Science and Engineering*, **60**, Article ID: 012002. https://doi.org/10.1088/1757-899x/60/1/012002

[6] Clark, A.E. (1988) Highly Magnetostrictive Rare Earth Compounds for High Power Acoustic Projectors. In: Hamonic, B. and Decarpigny, J.N., Eds., *Power Sonic and Ultrasonic Transducers Design*, Springer, 41-41. https://doi.org/10.1007/978-3-642-73263-8_5

[7] Kroeber, J., Audiere, J., Claude, R., Codjovi, E., Kahn, O., Haasnoot, J.G., *et al.* (1994) Spin Transitions and Thermal Hysteresis in the Molecular-Based Materials [Fe $(htrz)_2$ (Trz)](BF_4) and [$Fe(Htrz)_3$]$(BF_4)_2$. cntdot. H_2O (Htrz = 1, 2, 4-4H-Triazole; trz = 1, 2, 4-Triazolato). *Chemistry of Materials*, **6**, 1404-1412. https://doi.org/10.1021/cm00044a044

[8] Roubeau, O. (2012) Triazole-Based One-Dimensional Spin-Crossover Coordination Polymers. *Chemistry—A European Journal*, **18**, 15230-15244. https://doi.org/10.1002/chem.201201647

[9] Rotaru, A., Dugay, J., Tan, R.P., Guralskiy, I.A., Salmon, L., Demont, P., *et al.* (2013) Nano-Electromanipulation of Spin Crossover Nanorods: Towards Switchable Nanoelectronic Devices. *Advanced Materials*, **25**, 1745-1749. https://doi.org/10.1002/adma.201203020

[10] Ksenofontov, V., Gaspar, A. B. and Gütlich, P. (2004) Spin Crossover in Transition Metal Compounds III. *Topics in Current Chemistry*, **235**, 23-64. https://doi.org/10.1007/b95421

[11] Bousseksou, A., Molnár, G., Salmon, L. and Nicolazzi, W. (2011) Molecular Spin Crossover Phenomenon: Recent Achievements and Prospects. *Chemical Society Reviews*, **40**, 3313-3335. https://doi.org/10.1039/c1cs15042a

[12] Guionneau, P. (2014) Crystallography and Spin-Crossover. A View of Breathing Materials. *Dalton Trans.*, **43**, 382-393. https://doi.org/10.1039/c3dt52520a

[13] Grosjean, A., Négrier, P., Bordet, P., Etrillard, C., Mondieig, D., Pechev, S., *et al.* (2013) Crystal Structures and Spin Crossover in the Polymeric Material [$Fe(Htrz)_2$ (trz)](BF_4) Including Coherent-Domain Size Reduction Effects *European Journal of Inorganic Chemistry*, **2013**, 796-802. https://doi.org/10.1002/ejic.201201121

[14] Real, J.A., Gaspar, A.B., Niel, V. and Muñoz, M.C. (2003) Communication between Iron(II) Building Blocks in Cooperative Spin Transition Phenomena. *Coordination Chemistry Reviews*, **236**, 121-141. https://doi.org/10.1016/s0010-8545(02)00220-5

[15] Galet, A., Gaspar, A.B., Agusti, G., Muñoz, M.C., Levchenko, G. and Real, J.A. (2006) Pressure Effect Investigations on the Spin Crossover Systems {$Fe[H_2B(pz)_2]_2$(bipy)} and {$Fe[H_2B(pz)_2]_2$(phen)}. *European Journal of Inorganic Chemistry*, **2006**, 3571-3573. https://doi.org/10.1002/ejic.200600517

[16] Halcrow, M.A. (2011) Structure:Function Relationships in Molecular Spin-Crossover Complexes. *Chemical Society Reviews*, **40**, 4119-4142. https://doi.org/10.1039/c1cs15046d

[17] Bonhommeau, S., Guillon, T., Lawson Daku, L.M., Demont, P., Sanchez Costa, J., Létard, J., *et al.* (2006) Photoswitching of the Dielectric Constant of the Spin-Crossover Complex $[Fe(L)(CN)_2]\cdot H_2O$. *Angewandte Chemie International Edition*, **45**, 1625-1629. https://doi.org/10.1002/anie.200503252

[18] Bousseksou, A., Molnár, G., Real, J.A. and Tanaka, K. (2007) Spin Crossover and Photomagnetism in Dinuclear Iron(II) Compounds. *Coordination Chemistry Reviews*, **251**, 1822-1833. https://doi.org/10.1016/j.ccr.2007.02.023

[19] Halcrow, M.A. (2013) Spin-Crossover Materials: Properties and Applications. John Wiley & Sons.

[20] Konig, E., Ritter, G. and Kulshreshtha, S.K. (1985) The Nature of Spin-State Transitions in Solid Complexes of Iron(II) and the Interpretation of Some Associated Phenomena. *Chemical Reviews*, **85**, 219-234. https://doi.org/10.1021/cr00067a003

[21] Bau, R., Gütlich, P., Teller, R.G. and Gütlich, P. (1981) Spin Crossover in Iron(II)-Complexes. In: Bau, R., Gütlich, P., Teller, R.G., Eds., *Structure and Bonding*, Springer, 83-195. https://doi.org/10.1007/bfb0111269

[22] Bousseksou, A., Negre, N., Goiran, M., Salmon, L., Tuchagues, J.P., Boillot, M.L., *et al.* (2000) Dynamic Triggering of a Spin-Transition by a Pulsed Magnetic Field. *The European Physical Journal B*, **13**, 451-456. https://doi.org/10.1007/s100510050057

[23] Boillot, M., Chantraine, S., Zarembowitch, J., Lallemand, J. and Prunet, J. (1999) First Ligand-Driven Light-Induced Spin Change at Room Temperature in a Transition-Metal Molecular Compound. *New Journal of Chemistry*, **23**, 179-184. https://doi.org/10.1039/a809504c

[24] Varret, F., Bleuzen, A., Boukheddaden, K., Bousseksou, A., Codjovi, E., Enachescu, C., *et al.* (2002) Examples of Molecular Switching in Inorganic Solids, Due to Temperature, Light, Pressure, and Magnetic Field. *Pure and Applied Chemistry*, **74**, 2159-2168. https://doi.org/10.1351/pac200274112159

[25] Sorai, M. and Seki, S. (1974) Phonon Coupled Cooperative Low-Spin $^1A_1$high-Spin $^5T_2$ Transition in $[Fe(phen)_2(NCS)_2]$ and $[Fe(phen)_2(NCSe)_2]$ Crystals. *Journal of Physics and Chemistry of Solids*, **35**, 555-570. https://doi.org/10.1016/s0022-3697(74)80010-7

[26] Kahn, O. and Martinez, C.J. (1998) Spin-Transition Polymers: From Molecular Materials toward Memory Devices. *Science*, **279**, 44-48. https://doi.org/10.1126/science.279.5347.44

[27] Gütlich, P., Goodwin, H.A. and Hauser, A. (2004) Light-Induced Spin Crossover and the High-Spin → Low-Spin Relaxation. *Spin Crossover in Transition Metal Compounds*, **2**, 155-198.

[28] Spiering, H., Kohlhaas, T., Romstedt, H., Hauser, A., Bruns-Yilmaz, C., Kusz, J., *et al.* (1999) Correlations of the Distribution of Spin States in Spin Crossover Compounds. *Coordination Chemistry Reviews*, **190**, 629-647. https://doi.org/10.1016/s0010-8545(99)00109-5

[29] Gütlich, P., Gaspar, A.B. and Garcia, Y. (2013) Spin State Switching in Iron Coordination Compounds. *Beilstein Journal of Organic Chemistry*, **9**, 342-391. https://doi.org/10.3762/bjoc.9.39

[30] Nicolazzi, W., Pillet, S. and Lecomte, C. (2008) Two-Variable Anharmonic Model for

Spin-Crossover Solids: A Like-Spin Domains Interpretation. *Physical Review B*, **78**, Article 174401. https://doi.org/10.1103/physrevb.78.174401

[31] Boukheddaden, K., Shteto, I., Hôo, B. and Varret, F. (2000) Dynamical Model for Spin-Crossover Solids. I. Relaxation Effects in the Mean-Field Approach. *Physical Review B*, **62**, 14796-14805. https://doi.org/10.1103/physrevb.62.14796

[32] Jensen, K.P. and Cirera, J. (2009) Accurate Computed Enthalpies of Spin Crossover in Iron and Cobalt Complexes. *The Journal of Physical Chemistry A*, **113**, 10033-10039. https://doi.org/10.1021/jp900654j

[33] Kepp, K.P. (2013) Consistent Descriptions of Metal-Ligand Bonds and Spin-Crossover in Inorganic Chemistry. *Coordination Chemistry Reviews*, **257**, 196-209. https://doi.org/10.1016/j.ccr.2012.04.020

[34] Reeves, M.G., Tailleur, E., Wood, P.A., Marchivie, M., Chastanet, G., Guionneau, P., *et al.* (2021) Mapping the Cooperativity Pathways in Spin Crossover Complexes. *Chemical Science*, **12**, 1007-1015. https://doi.org/10.1039/d0sc05819j

[35] Shepherd, H.J., Gural'skiy, I.A., Quintero, C.M., Tricard, S., Salmon, L., Molnár, G., *et al.* (2013) Molecular Actuators Driven by Cooperative Spin-State Switching. *Nature Communications*, **4**, Article No. 2607. https://doi.org/10.1038/ncomms3607

[36] Cruz-Galván, A. and Olguín, J. (2025) Spin Crossover Iron(II) Complexes in Non-Hexacoordinate Geometries. *Trends in Chemistry*, **7**, 26-42. https://doi.org/10.1016/j.trechm.2024.11.001

[37] Harding, D.J., Harding, P. and Phonsri, W. (2016) Spin Crossover in Iron(III) Complexes. *Coordination Chemistry Reviews*, **313**, 38-61. https://doi.org/10.1016/j.ccr.2016.01.006

[38] Nicolazzi, W. and Bousseksou, A. (2018) Thermodynamical Aspects of the Spin Crossover Phenomenon. *Comptes Rendus. Chimie*, **21**, 1060-1074. https://doi.org/10.1016/j.crci.2018.10.003

[39] Tokarev, A., Salmon, L., Guari, Y., Molnár, G. and Bousseksou, A. (2011) Synthesis of Spin Crossover Nano-Objects with Different Morphologies and Properties. *New Journal of Chemistry*, **35**, 2081. https://doi.org/10.1039/c1nj20218a

[40] Gütlich, P., Hauser, A. and Spiering, H. (1994) Thermal and Optical Switching of Iron(II) Complexes. *Angewandte Chemie International Edition in English*, **33**, 2024-2054. https://doi.org/10.1002/anie.199420241

[41] Decurtins, S., Gütlich, P., Köhler, C.P., Spiering, H. and Hauser, A. (1984) Light-Induced Excited Spin State Trapping in a Transition-Metal Complex: The Hexa-1-Propyltetrazole-Iron (II) Tetrafluoroborate Spin-Crossover System. *Chemical Physics Letters*, **105**, 1-4. https://doi.org/10.1016/0009-2614(84)80403-0

[42] Buhks, E., Navon, G., Bixon, M. and Jortner, J. (1980) Spin Conversion Processes in Solutions. *Journal of the American Chemical Society*, **102**, 2918-2923. https://doi.org/10.1021/ja00529a009

[43] Sasaki, N. and Kambara, T. (1982) The Effect of a Magnetic Field on the High Spin to or from Low-Spin Transitions in Ferrous and Ferric Compounds. *Journal of Physics C: Solid State Physics*, **15**, 1035-1071. https://doi.org/10.1088/0022-3719/15/5/021

[44] Gütlich, P., Bousseksou, A. and Spiering, H. (2004) Spin Crossover Phenomena. *Topics in Current Chemistry*, **233**.

[45] Hauser, A. (2004) Light-Induced Spin Crossover and the High-Spin → Low-Spin Relaxation. In: Gütlich, P. and Goodwin, H.A., Eds., *Spin Crossover in Transition Metal Compounds II*, Springer, 155-198. https://doi.org/10.1007/b95416

[46] Kim, H.S., Lee, S.H., Yoo, S. and Adachi, C. (2024) Understanding of Complex Spin Up-Conversion Processes in Charge-Transfer-Type Organic Molecules. *Nature Communications*, **15**, Article No. 2267. https://doi.org/10.1038/s41467-024-46406-5

[47] Onsager, L. (1931) Reciprocal Relations in Irreversible Processes. I. *Physical Review*, **37**, 405-426. https://doi.org/10.1103/physrev.37.405

[48] Onsager, L. (1931) Reciprocal Relations in Irreversible Processes. II. *Physical Review*, 38, Article 2265.

[49] Carnot, S. (1872) Réflexions sur la puissance motrice du feu et sur les machines propres à développer cette puissance. *Annales Scientifiques de l'École Normale Supérieure*, **1**, 393-457. https://doi.org/10.24033/asens.88

[50] Boltzmann, L. (1872) Weitere studien über das wärmegleichgewicht unter gasmolekülen. Vol. 66, Aus der kk Hot-und Staatsdruckerei, 275-370.

[51] Parker, S.P. (1993) Encyclopedia of Physics. 2nd Edition, McGraw Hill.

[52] Chapman, S. (1937) Boltzmann's *H*-Theorem. *Nature*, **139**, 931-931. https://doi.org/10.1038/139931a0

[53] Tolman, R.C. (1938) The Principle of Statistical Mechanics. Oxford at the Clarendon Press. https://archive.org/details/ThePrinciplesOfStatisticalMechanicsTolmanOxfordAtTheClarendonPress1938

[54] Gibbs, J.W. (1902) Elementary Principles in Statistical Mechanics: Developed with Especial Reference to the Rational Foundations of Thermodynamics. C. Scribner's Sons. https://doi.org/10.5962/bhl.title.32624

[55] von Neumann, J. (2010) Proof of the Ergodic Theorem and the H-Theorem in Quantum Mechanics. *The European Physical Journal H*, **35**, 201-237. https://doi.org/10.1140/epjh/e2010-00008-5

[56] Von Neumann, J. (1955) Mathematical Foundations of Quantum Mechanics. Beyer, R.T., Trans, Princeton University Press.

[57] Evans, D.J., Cohen, E.G.D. and Morriss, G.P. (1993) Probability of Second Law Violation in Shearing Steady States, *Physical Review Letters*, **71**, 2401-2404. https://pdfs.semanticscholar.org/697a/31eace27d3b0096700709d83d5f3bd8f1733.pdf

[58] Evans, D.J. and Searles, D.J. (1996) Causality, Response Theory, and the Second Law of Thermodynamics. *Physical Review E*, **53**, 5808-5815. https://doi.org/10.1103/physreve.53.5808

[59] Evans, D.J. and Searles, D.J. (2019) The Fluctuation Theorem. *Advances in Physics*, **51**, 1529-1585. https://pdfs.semanticscholar.org/470a/4e148c2ba7aa0f6d48d455d9a854db2a1da2.pdf

[60] Crooks, G.E. (1999) Entropy Production Fluctuation Theorem and the Nonequilibrium Work Relation for Free Energy Differences. *Physical Review E*, **60**, 2721-2726. https://doi.org/10.1103/physreve.60.2721

[61] Levy, G.S. (2019) Loschmidt's Paradox, Extended to CPT Symmetry, Bypasses Second Law. *Journal of Applied Mathematics and Physics*, **7**, 3140-3175. https://doi.org/10.4236/jamp.2019.712221 https://www.scirp.org/journal/paperinformation.aspx?paperid=97267

[62] Levy, G.S. (2023) An Overview of the $E \times B$ Thermoelectric Effect. *MRS Advances*, **8**, 113-118. https://doi.org/10.1557/s43580-023-00521-5

[63] Levy, G.S. (2022) The $E \times B$ Thermoelectric Effect, Video Presentation. https://youtu.be/CBenek-3MGs

[64] Levy, G.S. (2023) The $E \times B$ Thermoelectric Effect Bypasses the Second Law. ResearchGate. https://doi.org/10.13140/RG.2.2.29199.56483

[65] Levy, G.S. (2021) $E \times B$ Drift Thermoelectric Energy Generation Device. US Patent No. 10971669.

[66] Levy, G.S. (2024) $E \times B$ Drift Thermoelectric Energy Device. PCT Patent Application No. PCT/US2024/024668.

[67] Lee, J.W. (2024) Type-B Energetic Processes: Their Identification and Implications. *Symmetry*, **16**, Article 808. https://doi.org/10.3390/sym16070808

[68] Lee, J.W. (2022) Type-B Energy Process: Asymmetric Function-Gated Isothermal Electricity Production. *Energies*, **15**, Article 7020. https://doi.org/10.3390/en15197020

[69] Lee, J.W. (2022) Type-B Energetic Processes and Their Associated Scientific Implications. *Journal of Scientific Exploration*, **36**, 484-492. https://doi.org/10.31275/20222517

[70] Sheehan, D.P. (2023) A Self-Charging Concentration Cell: Theory. *Batteries*, **9**, Article 372. https://doi.org/10.3390/batteries9070372

[71] Sheehan, D.P., Hebert, M.R. and Keogh, D.M. (2022) Concentration Cell Powered by a Chemically Asymmetric Membrane: Experiment. *Sustainable Energy Technologies and Assessments*, **52**, Article ID: 102194. https://doi.org/10.1016/j.seta.2022.102194

[72] Sheehan, D.P., Garamella, J.T., Mallin, D.J. and Sheehan, W.F. (2012) Steady-State Nonequilibrium Temperature Gradients in Hydrogen Gas-Metal Systems: Challenging the Second Law of Thermodynamics. *Physica Scripta*, **151**, Article ID: 014030. https://doi.org/10.1088/0031-8949/2012/t151/014030

[73] Nikulov, A.V. (2021) Dynamic Processes in Superconductors and the Laws of Thermodynamics. *Physica C*: *Superconductivity and Its Applications*, **589**, Article ID: 1353934. https://doi.org/10.1016/j.physc.2021.1353934

[74] Gurtovoi, V.L., Antonov, V.N., Exarchos, M., Il'in, A.I. and Nikulov, A.V. (2019) The Dc Power Observed on the Half of Asymmetric Superconducting Ring in Which Current Flows against Electric Field. *Physica C*: *Superconductivity and Its Applications*, **559**, 14-20. https://doi.org/10.1016/j.physc.2019.01.009

[75] Fu, X. and Fu, Z. (2016) Realization of Maxwell's Hypothesis: A Heat-Electric Conversion in Contradiction to the Kelvin Statement. arXiv: physics/0311104.

[76] Kondo, S., Kameyama, M., Imaoka, K., Shimoi, Y., Mathevet, F., Fujihara, T., *et al.* (2024) Organic Thermoelectric Device Utilizing Charge Transfer Interface as the Charge Generation by Harvesting Thermal Energy. *Nature Communications*, **15**, Article No. 8115. https://doi.org/10.1038/s41467-024-52047-5

[77] Dexter Magnetic Technologies (2025) Dipoles, Halbach & Stelter Arrays. https://www.dextermag.com/products/magnetic-assemblies/dipoles-halbach-stelter-arrays/

[78] Zhang, B. and Hatch, G.P. (2009) Field Analysis and Comparison of Several Permanent Magnet Dipole Structures. *IEEE Transactions on Magnetics*, **45**, 4395-4398. https://doi.org/10.1109/tmag.2009.2024428

[79] Wikipedia (2025) Solar Irradiance. https://en.wikipedia.org/wiki/Solar_irradiance

[80] Shockley, W. and Queisser, H. (2018) Detailed Balance Limit of Efficiency of *p-n* Junction Solar Cells. *Renewable Energy*, Routledge, 35-54.

[81] Feynman, R.P. (2025) Azquotes. https://www.azquotes.com/quote/1217348

Appendix 1. List of Symbols

μ_{magn}	Magnetic moment
A	Area
B	Magnetic field
D	Diffusion constant
E	Energy
f	Fermi-Dirac distribution
F_B	Force produced by the magnetic field
F_{conv}	Convective force
F_{load}	Backward force due to load
F_{magn}	Force produced by the magnetic potential
F_{visc}	Backward force due to viscous processes
F_{visc_hyst}	Backward force due to hysteretic viscous drag
F_{visc_Newton}	Backward force due to Newtonian viscous processes
g	Gravity's acceleration
h	Height of fluid column
k_B	Boltzmann's constant
K_m	Stereo-magnetostrictive volume ratio modulus
K_p	Pressure volume ratio modulus
L	Length of convection loop
m	Mass of a small fluid volume undergoing convection
n	Volume fraction of magnetostrictive particles
p	Pressure
p_{conv}	Convective head pressure
P_{load}	Power transmitted to the load
p_{visc}	Backward pressure due to viscous processes
p_{visc_Newton}	Backward pressure due to Newtonian viscous processes
Q	Heat
Q_{Flow}	Fluid flow
r	Radius of convection tube
$r_{molecule}$	Radius of molecule
s	Magnetostrictive strain
S_A	Conventional entropy
S_B	Anomalous entropy
T	Temperature
t	Time
V	Volume
$v_{Brownian}$	Brownian drift velocity
v_{drift}	Drift velocity due to field gradient
v_{Flow}	Convective speed of fluid
W	Work energy
Δh	Pressure head caused by a difference in density
η	Viscosity
ρ	Density
τ_{shear}	Shear stress
τ_{yield}	Yield stress

Appendix 2. Separation of SCO Molecules by the Magnetic Field

This analysis addresses the question of whether the magnetic field used in this thought experiment results in the separation of the spin cross-over (SCO) molecules from the solution. The answer is "no" for the following reason.

The SCO molecules (e.g., Fe(II) or Fe(III) complexes) exist in two states: low spin (LS) and high spin (HS). They differ on how many unpaired electrons they have. LS have fewer unpaired electrons and a lower magnetic moment. HS which are induced by a magnetic field have more unpaired electrons and a higher magnetic moment. The force produced by a magnetic field B on an HS molecule with magnetic moment μ_{magn} in an inhomogeneous field B is:

$$\boldsymbol{F}_{magn} = \nabla\left(\boldsymbol{\mu}_{magn} \cdot \boldsymbol{B}\right) \tag{64}$$

This magnetic force causes the molecules to drift with velocity v and to experience a drag force $F_{drag} = -F_{magn}$. This force depends on the dynamic viscosity η of the fluid, and on the radius $r_{molecule}$ of the molecules in accordance with Stoke's law:

$$\boldsymbol{F}_{drag} = -6\pi\eta r_{molecule}\boldsymbol{v}_{drift} = -\boldsymbol{F}_{magn} \tag{65}$$

Therefore, the drift velocity of a molecule in a magnetic field is:

$$\boldsymbol{v}_{drift} = \frac{\nabla\left(\boldsymbol{\mu}_{magn} \cdot \boldsymbol{B}\right)}{6\pi\eta r_{molecule}} \tag{66}$$

Assuming the following:

- SCO molecules with a magnetic moment of $\mu = 4$ Bohr magnetons $= 4 \times 9.27 \times 10^{-24} = 3.71 \times 10^{-23}$J/T (reasonable assumption for a spin cross-over molecule).
- A field gradient of $\nabla B = 10$ T/m.
- The viscosity of water $\eta = 1 \times 10^{-3}$ Pa·s.
- A hydrodynamic radius of molecule $r = 1 \times 10^{-9}$ m.

Then, the magnetic drift velocity is:

$$\boldsymbol{v}_{drift} = 19.7 \times 10^{-12}\ \mathrm{m/s} \tag{67}$$

This drift velocity needs to be compared with the displacement caused by Brownian motion. At a temperature of 300 K, the diffusive coefficient for a particle of radius $r_{molecule}$ is:

$$D = \frac{k_B T}{6\pi\eta r_{molecule}} \tag{68}$$

and the characteristic random displacement over a time t due to diffusion is:

$$\left\langle x^2 \right\rangle^{1/2} = \sqrt{2Dt} = \sqrt{\frac{2k_B T}{6\pi\eta r_{molecule}} t} \tag{69}$$

Assuming $T = 300$ K, the displacement over one second is

$$\left\langle x^2 \right\rangle^{1/2} = 20.96 \times 10^{-6}\ \mathrm{m} \tag{70}$$

In summary, random thermal motion displaces the molecule ~20 microns in 1

second, while the magnetic drift moves it only 20 picometers—a million times smaller. Therefore, separation of the molecules from the solution by the magnetic field is not a concern.

Appendix 3. Clarification of Time-Reversal Asymmetry

A common source of confusion in discussing magnetic-field effects and time-reversal symmetry is the failure to distinguish between the **frame of the experimenter** and the **frame of the experiment**. The naïve approach is to argue that an experiment involving charged particles or magnetic material in a magnetic field is time-reversal **symmetric** because the field flips direction and, therefore, the behavior of the particles or material is invariant with time-reversal.

In actuality, one should distinguish three participators in such an experiment:

1) The experimenter with his own frame of reference. He is equipped with measuring instruments such as a magnetometer and a clock which are unaffected by time reversal.

2) The experiment itself with its own frame of reference in which time is reversed.

3) The magnetic field and the mechanism that produces it, for example moving charges.

In which frame should the magnetic field and its source be located? The answer is that it does not matter.

1) If the magnetic field is placed in the experimenter's frame, the field remains invariant, and the experiment is observed to be time-reversal asymmetric.

2) If the field is placed in the frame of the experiment, it flips direction, *resulting in the whole experiment being observed as time-reversal asymmetric*.

In either configuration, *the presence of the field itself, not in which frame it is placed*, breaks the time-reversal symmetry assumed in H-theorem derivations. This outcome is a consequence of the CPT symmetry of the electromagnetic field evidenced by the right-hand rule. In summary, the T-odd asymmetry of the magnetic field is invariant under a time-reversal frame transformation and is not covered by the H-theorem. This is the reason Onsager excluded it from his reciprocals.

Table 1 and Table 2 summarize a series of time-reversal thought experiments involving a test particle and a field-causing "particle". For simplicity, we assume that the charge on the field-causing particle is much larger than the charge on the test particle (*i.e.*, the field-causing particle may consist of a body such as a wire comprised of multiple elementary charged particles).

The tests highlight the CPT properties of these particles using the right-hand rule. The experiments in Table A1 involve expressing CT conjugation and keeping P constant. Those in Table A2 involve expressing PT conjugation and keeping C constant. In every instance, the time reversed magnetic field produces a T-odd behavior of the test particle, thereby breaking their time reversal symmetry.

Table of symbols:

⊕	Positive charge
⊖	Negative charge
⊙	Field "out of paper"
⊗	Field "into paper"
↻	Clockwise
↺	Counterclockwise
Red	Invariant quantity
Blue	variable quantity

Table A1. Breaking of time-reversal symmetry by CPT symmetry of magnetic field.

Set up experiments with CT conjugates, P invariant			
		Frame of observer	**Frame of experiment**
Experiment 1: - Field-causing particle in observer's frame producing ⊙ field. - Test particle in observer's frame subjected to ⊙ field. - This is the baseline experiment without time reversal.	Field-causing particle	Charge ⊕ Parity ⊙ Time ↺	
	Test particle	Charge ⊕ Parity ⊙ Time ↺	
Experiment 2: - Field-causing particle in observer's frame producing field ⊙ - Test particle in −T (time reversal) experiment flips C to ⊖ leaves P at ⊙. Left hand rule applies to ⊖ particle subjected to ⊙ field. - Result: test particle breaks time reversal symmetry.	Field-causing particle	Charge ⊕ Parity ⊙ Time ↺	
	Test particle		Charge ⊖ Parity ⊙ Time ↻
Experiment 3: - Field-causing particle in −T (time reversal) experiment flips C to ⊖, leaves P at ⊙. - Test particle in observer frame. Right hand rule applies to particle subjected to ⊙ field. - Result: Field-causing particle breaks time reversal symmetry.	Field-causing particle		Charge ⊖ Parity ⊙ Time ↻
	Test particle	Charge ⊕ Parity ⊙ Time ↺	
Experiment 4: - Field-causing particle in −T (time reversal) experiment flips C to ⊖ leaves P at ⊙. - Test particle in −T (time reversal) experiment flips C to ⊖, leaves P at ⊙. Left hand rule applies to ⊖ particle subjected to ⊙ field. - Result: both particles break time reversal symmetry.	Field-causing particle		Charge ⊖ Parity ⊙ Time ↻
	Test particle		Charge ⊖ Parity ⊙ Time ↻

Table A2. Breaking of time-reversal symmetry by CPT symmetry of magnetic field.

Set up experiments with PT conjugates, C invariant		Frame of observer	Frame of experiment
Experiment 1: - Field-causing particle in observer's frame producing field ⊙. - Test particle in observer's frame subjected to ⊙ field. - This is the baseline experiment without time reversal.	Field-causing particle	Charge ⊕ Parity ⊙ Time ↺	
	Test particle	Charge ⊕ Parity ⊙ Time ↺	
Experiment 2: - Field-causing particle in observer's frame producing field ⊙ - Test particle in −T (time reversal) experiment flips P to ⊗ leaves C at ⊕. Left hand rule applies to ⊗ particle subjected to field ⊙ - Result: test particle breaks time reversal symmetry.	Field-causing particle	Charge ⊕ Parity ⊙ Time ↺	
	Test particle		Charge ⊕ Parity ⊗ Time ↻
Experiment 3: - Field-causing particle in −T (time reversal) experiment flips P to ⊗ leaves C at ⊕. - Test particle in observer's frame. Left hand rule applies to particle subjected to ⊗ field. - Result: both particles break time reversal symmetry.	Field-causing particle		Charge ⊕ Parity ⊗ Time ↻
	Test particle	Charge ⊕ Parity ⊙ Time ↻	
Experiment 4: - Field-causing particle in −T (time reversal) experiment flips P to ⊗, leaves C at ⊕. - Test particle in −T (time reversal) experiment flips P to ⊗, leaves C at ⊕. Left hand rule applies to ⊗ particle subjected to ⊗ field. (Parity reversal is applied once because it affects both particles simultaneously. End result is consistent ↻ for both particles). - Results: both particles break time reversal symmetry.	Field-causing particle		Charge ⊕ Parity ⊗ Time ↻
	Test particle		Charge ⊕ Parity ⊗ Time ↻

Appendix 4. The $E \times B$ Thermoelectric Effect

Possibly, the simplest example of CPT symmetry is the $E \times B$ drift. In the presence of an electric field E and a magnetic field B perpendicular to each other, charged particles follow cycloids moving perpendicular to both fields in the $E \times B$ direction, drifting with velocity:

$$v_{Drift} = \frac{E \times B}{|B|^2} \tag{71}$$

Reversing time produces an antisymmetric motion along $-E \times B$, clearly distinguishable from its motion in forward time. The total kinetic and potential energy of a particle remains constant but its position changes along the drift axis. This drift results in shrinking in the uncertainty of the volume occupied by the particle. This "free compression" corresponds to an increase in information and a decrease

in entropy which is not accounted for by conventional thermodynamics formulations such as the H-theorem because it is time-reversal asymmetric. The return path is devoid of magnetic field to ensure cyclic operation. The $E \times B$ drift is the basis for the $E \times B$ thermoelectric effect [62]-[66].

Appendix 5. Isothermal Engine Using Solid Joule Magnetostriction

As shown in this paper, an engine using a stereo-magnetostrictive fluid is relatively easy to implement. However, other kinds of magnetostrictive engines are possible using solid Joule magnetostrictive materials that change shape but not volume. For example, such an engine could be in the form of a wheel mounted with bearings on a horizontal axle and with spokes comprised of Joule magnetostrictive solid material. In the absence of any magnetic field, the wheel would be in equilibrium, its center of gravity exactly at the center of the axle, and it would not turn. However, if one of its sides were exposed to a field, the spokes would elongate on that side, causing a shift in the center of gravity away from the axle, and causing the wheel to turn. One should note that the magnetic force acting on the wheel is perpendicular to gravity and causes rotation indirectly not by horizontally pulling on the spokes but through the magnetostrictive change in the length of the spokes and the vertical pull of gravity. From a practical point of view, such a solid magnetostrictive engine would probably be more difficult to implement than the fluid engine described in this paper. Being ferromagnetic, the Joule magnetostrictive materials would be strongly attracted by the field along the horizontal direction. The resulting torque would then complicate the design of the bearings. It would require them to be strong enough to withstand the horizontal torque yet have extremely low friction to allow the wheel to turn under the vertical influence of gravity.